ENVIRONMENTAL AND ECONOMIC ANALYSIS OF COLD IRONING USING RENEWABLE HYBRID SYSTEMS

Onur Yuksel[1,2], Murat Bayraktar[2], Alper Seyhan[3]

o.yuksel@ljmu.ac.uk, ORCID: 0000-0002-5728-5866
bayraktarmurat@beun.edu.tr, ORCID: 0000-0001-7252-4776
alperseyhan@beun.edu.tr, ORCID: 0000-0003-3707-6706

[1]Liverpool Logistics Offshore and Marine Research Institute (LOOM), Faculty of Engineering, Liverpool John Moores University, Byrom Street, Liverpool L3 3AF, UK
[2]Zonguldak Bülent Ecevit University, Maritime Faculty, Marine Engineering Department, 67300, Zonguldak, Türkiye
[3]Zonguldak Bülent Ecevit University, Maritime Faculty, Maritime Transportation and Management Engineering Department, 67300, Zonguldak, Türkiye

ABSTRACT

This paper investigates shore-based photovoltaic (PV)/proton exchange membrane fuel cell (PEMFC) and PV/Battery renewable energy (RE) plants for cold-ironing (CI) configurations. The hydrogen for PEMFCs is produced in ammonia (NH_3) electrolyser by the PV panel-sourced electricity using green, blue or grey NH_3 as the feedstock. The system models based on PV technology are developed using minimum, average, and maximum monthly irradiation levels. The environmental and economic analyses benchmark CI based on grid/RE electricity with onboard electricity generation using diesel and dual-fuel systems with light fuel oil (LFO) and liquefied natural gas (LNG). Results show that LNG usage in the ship electrification plant reduces equivalent carbon dioxide (CO_{2e}) by 14.27%, sulphur oxides by 90.79%, and nearly eliminates other emissions. Using grid electricity as the CI source cuts CO_{2e} by 58.92%, while the PV/Battery system reduces it by 80.73% to 85.82%, depending on irradiation. The PV/PEMFC system with green NH_3 achieves the highest CO_{2e} reduction (99.92%-100%), while blue NH_3 provides the second-largest decrease (97.46%-97.54%). The grid electricity CI has the shortest payback period (PBP) at 2.06 years and a levelized cost of energy (LCOE) of $186.92/MWh. The PV/Battery system has an LCOE of $174.67 to $196.52/MWh and a PBP of 6.98 to 8.78 years. The PV/PEMFC system using grey NH_3 shows a PBP of 7.78 years, rising to 9.01 years with blue NH_3 and 23.69 years with green NH_3. LCOE of the PV/PEMFC ranges from $129-$184.18/MWh with grey NH_3, $151.94-$233.36/MWh with blue, and $177.09-$359.89/MWh with green NH_3.

Keywords: Greenhouse gases (GHG), Cold ironing (CI), Photovoltaic (PV) Panel, Proton Exchange Membrane Fuel Cell (PEMFC), Ammonia (NH_3) electrolysis.

NOMENCLATURE

A_P: one solar panel area
AC: Alternative current
AE: Auxiliary engine
AMS: Automatic Mooring System
C_{flow}: Annual net income
C_{fuel}: Fuel cost
$C_{O\&M}$: Operation and maintenance cost
C_{plant}: Total investment cost.
CEPCI: Chemical Engineering Plant Cost Index
CH_4: Methane
CI: Cold Ironing
CII: Carbon intensity indicator
C_o: Coefficient operational
C_u: Coefficient upstream
CO_2: Carbon dioxide
CO_{2e}: Equivalent carbon dioxide
DC: Direct current
DF: Dual fuel
E: energy output of one solar panel
E_d: Energy demand of the vessels
EEXI: Energy Efficiency Existing Ship Index
EU ETS: European Union Emission Trading System
FC: Fuel cell
GHG: Greenhouse gas
GT: Gross Tonnage
H_2: Hydrogen
H_a: Solar irradiation
LCOE: Levelized cost of energy
LFO: Light fuel oil
LNG: Liquefied natural gas
LOA: Length Overall
MDE: Marine diesel engine
ME: Main engine
MW: Megawatt
MPPT: Maximum PowerPoint Tracker
NH_3: Ammonia
NoG: Number of Generators
N_2O: Nitrous Oxide
NO_x: Nitrous oxide
O&M: Operational and Maintenance
P_{gen}: Total generated power
P_{PEMFC}: PEMFC power
P_r: Performance ratio
PBP: Payback period
PEMFC: Proton exchange membrane fuel cell
PM: Particulate matter
P&T: Pressure and Transfer
PV: Photovoltaic
r: Discount rate in LCOE calculation
R: Independent result in the uncertainty analysis
RE: Renewable energy
SFC: Specific fuel consumption
SO_x: Sulphur oxide
t: System Lifetime
t_{op}: Operation time
U: Fractional uncertainty
U_R: Combined uncertainty
USD: United States dollar ($)
x: Independent value in the uncertainty analysis
VOC: Volatile organic compound

Greek Symbols

η: PV panel efficiency

1. INTRODUCTION

Maritime transportation carries out over 80% of global transportation by volume (UNCTAD, 2023) and is crucial for a sustainable economy however it accounts for 2.9% of global greenhouse gas (GHG) emissions (DNV, 2024; EuropeanCommission, 2024). A remarkable part of these GHGs is generally emitted from ship operations in ports either cruising or berthing. Unlike cruising operation mode, ships emit GHG mostly from the generators which generate electricity for hotel load and onboard devices during the waiting period in the port (Bakar et al., 2022). Using an onshore-based power to meet the electricity demand of the vessel can potentially mitigate the GHGs resulting from berthed ships. The process referred to as cold ironing (CI) can decrease the reliance on fossil fuels with the addition of renewable energy (RE) systems which is why it can be a crucial innovation in the shore facilities (Kelmalis et al., 2024). CI allows the energy needed on the ship during the berthing period to be supplied from shore-based electrical sources rather than onboard generators (Abu Bakar et al., 2023). Although CI has been long employed in naval ships, its prevalence in commercial shipping has significantly increased over the last two decades, particularly in large-scale ports (Wartsila, 2024). Given the high population density in regions near the world's major ports, the implementation of CI will have a substantial positive impact on air quality (Kılıç et al., 2020; Tang et al., 2018).

CI, which greatly aids in reducing greenhouse gas emissions, possesses significant potential for fostering the development of green ports and decarbonisation strategies worldwide (Tang et al., 2018). Despite the feasibility of implementing CI in numerous ports, the high initial investment and ship retrofitting costs cause hesitation among stakeholders both on the shore and shoreside. Therefore, stakeholders need to integrate and cooperate to ensure sustainable maritime transportation. The integration and cooperation process can be expedited through government incentives and international regulations (Abu Bakar et al., 2023; Glavinović et al., 2023). In addition to implementations like the European Union Emission Trading System (EU ETS), emerging technologies could shorten the long payback period of CI and make it easier to overcome retrofitting challenges yielding accelerating CI applications worldwide (Abu Bakar et al., 2023; Piccoli et al., 2021). The increased number of ships arriving and their berthing durations at the port can heighten the demand for CI applications. Therefore, determining the optimal capacity for cold ironing to meet energy demands is essential; otherwise, power outages may occur, resulting in economic losses and port congestion (Abu Bakar et al., 2024; Qiu et al., 2022). The duration ships spend berthed at the port is determined by factors encompassing ship types, dimensions, arrival times, operational modes, and capacity indices (Bakar et al., 2022).

In particularly large-scale ports, the main grid may be insufficient to meet the electricity demands of ships berthed in the port. CI can be supported with microgrids including energy storage systems and RE sources to eliminate the main grid burden, particularly in peak energy consumption intervals of the ships (Abu Bakar et al., 2024; Tang et al., 2018). Additionally, these hybrid systems provide benefits in terms of both cost and health because electricity for the main grid is generally produced from fossil sources (Qiu et al., 2022; Tang et al., 2018). CI applications, particularly those integrated with smart systems, offer highly promising potential and drive gains to higher levels (Prousalidis et al., 2014). Batteries, photovoltaic (PV) panels, wind turbines, and fuel cells (FCs) are the most proposed ones to supply CI systems within the context of alternative and RE resources. Apart from environmental impact, significant cost savings are achieved, particularly in countries where unit energy production is economical (Piccoli et al., 2021; Qiu et al., 2022). Electrical energy generated from renewable sources is exported to support the main grid in addition to meeting the energy needs of ships (Kelmalis et al., 2024).In addition to reducing GHG emissions, turning off diesel generators during ships' docking periods diminishes both noise and vibration levels (Abu Bakar et al., 2024; Canepa et al., 2023).

1.1. Literature Review

Various research papers to investigate the CI applications supported with RE systems including solar and wind applications on economic, environmental and availability aspects have been conducted. A literature review encompassing the studies between 2020 and 2024 has been performed to detect the trend and research gap about the CI applications. In 2020 and 2021, the number of studies started to increase as the CI as a concept was getting more popular. The selected studies related to the motivation of this paper from these years have been examined in the review. Kılıç et al. (2020) calculated the emissions and resulting potential costs in Iskenderun Port and evaluated the CI as a solution to prevent these outcomes. The findings demonstrated that an RE-based CI application can prevent the annual emission cost of $23,000,000. Piccoli et al. (2021) performed an environmental analysis and regulatory assessment of CI implementation for different ports located in the Adriatic region. Depending on the port profile and EU ETS, the CI implementation has been found as a beneficial investment. Caprara et al. (2021) reported a CI application in a cruise terminal applying batteries and RE plants which has a capacity of 9.3 MW to meet the hotel and operational load of the cruise ships. The main benefits were turning off ship engines reducing emissions, noise, and vibrations, and improving air quality, marine life, and passenger comfort while meeting cruise ships' high power demands was the main challenge. Vahabzad et al. (2021) investigated a PV and diesel generator hybrid CI facility on a case study port. Results showed that the total cost reduction of the hybrid power system in various case studies was only 1% to 2% without CI services but increased to 6% to 7% with the addition of CI facilities.

In 2022, the number of RE utilisation in CI applications has increased compared to 2020 and 2021. Bakar et al. (2022) determined the optimum system design and size of RE-utilised CI integration to the Aalborg Port. The economic and environmental aspects were evaluated and the PV/wind/converter hybrid system was detected as the optimal design for the reference port. Qiu et al. (2022) proposed a tariff determination process for CI services targeting electric marine vessels. It was discovered that the suggested method encourages more effectively all-electric ships to implement emission control and power congestion management compared to the existing approaches. Sifakis et al. (2022) presented a CI approach involving a hydrogen (H_2) RE plant in the port of Milos. The proposed system can reduce the energy cost by 41.3% compared to the base case. Caprara et al. (2022) assessed the PV/Wave Energy/battery-based CI infrastructure in the port of Civitavecchia cruise terminal. Results indicated that the battery packs, sized at 8.73 MW and 121.25 MWh, support the port grid by optimising RE use, reducing energy costs through load shifting, and meeting Cruise Ships' CI load while acting as a backup when generators are offline.

In 2023, Glavinović et al. (2023) conducted a survey study targeting the port authorities and experts about CI integration in Croatian Ports. The investigation revealed that every expert questioned supported the idea of using cold ironing technology in state-owned ports. To achieve sustainable implementation, significant investments and finance requirements must be considered. Seyhan et al. (2023) assessed emission reduction rates when the Automatic Mooring System (AMS) and CI were applied individually and jointly at a port in Izmit Bay. Using only AMS, CO_2, nitrogen oxide (NO_x), PM, and sulphur oxide (SO_x)emissions decreased by 3.58%, 3.55%, 11.19%, and 3.45%, respectively. With CI alone, reductions were 21.21% for CO2, 88.85% for NOx, 47.17% for particulate matter (PM), and 2.33% for SO_x. When both systems were combined, emission reductions increased to 24.79% for CO_2, 92.40% for NOx, 58.37% for PM, and 5.78% for SO_2. Compared to different systems, CI also mitigated a larger amount of emissions in the port. Vakili and Ölçer (2023) evaluated the potential of solar, wind power, and generator usage in six stand-alone and grid-connected systems for a major Philippine port through 1,423 simulations using smart grid optimisation software and a Python program. Grid-connected systems proved more cost-effective and environmentally friendly than stand-alone systems, with wind power systems having the lowest Levelized Cost of Electricity (LCOE) at $0.081/kWh. Yfantis et al. (2023) examined an integrated CI configuration involving RE and liquefied natural gas (LNG)-fuelled gas turbines. The proposed system tracked sustainability progress by accurately estimating and monitoring GHG emissions, advising users on whether re-routing or CI is more efficient for fuel savings. When properly implemented, CI significantly improved air quality.

Finally, in 2024, Abu Bakar et al. (2024) studied a novel energy management strategy involving two stages for a RE-based CI application. Outcomes depicted a 28% reduction in port emissions and a 38.44% CO_2 deduction in ship electricity generation plant emissions. Kelmalis et al. (2024) presented a case study for the RE-utilised CI system in the port of Lesvos Island. Their design involved a wind energy plant generating an annual 72,080 MWh providing a remarkable amount of CO_2.Şenol and

Seyhan (2024) conducted a feasibility study at a new port using the HOMER software, the Wind Turbine/PV/battery/diesel scenario achieved the lowest LCOE and the highest renewable energy share. Enea and Mastrilli (2024) analysed PV and tidal energy plants combined with an LNG storage facility in a CI infrastructure in the Strait of Messina ports as the case study. The cost and CO_2 emission reduction were achieved by the proposed design. Frković et al. (2024) assessed the ship-to-shore or CI applications' impact on the decarbonisation of ships at berth. Sustainable ship electrification required fully renewable energy regarding outcomes while integrating CI power RE reduced excess energy, CO_2 emissions, and operating costs, enhancing port sustainability. Binot et al. (2024) proposed a novice approach to integrated optimisation of sizing and energy management of CI microgrids. The case study findings showed that the microgrid significantly reduced CO_2 emissions by 1.58 times, but increased costs compared to the current design using marine diesel generators.

1.2. Research Gap and Motivation

The literature review on the environmental and economic investigation of CI integration in the port facilities depicted that PV panels and wind systems have been the most studied RE systems. While it has only been used to meet just a small part of the electrical demand, some studies concentrate on integrating the FC system into RE systems. There has been a research gap in the environmental and economic feasibility analysis of an FC-CI system to meet large electrical demands using H_2. The research question of this study involves if the based FC using H_2 from different sources of ammonia (NH_3) as feedstock carries out the CI operation, how will it impact the operational upstream GHG and its economic feasibility? This study aims to investigate a shore-based PV//Proton Exchange Membrane FC (PEMFC) hybrid RE plant for CI application in a reference port integrated with an NH_3 cracking system to generate H_2 for PEMFCs. An alkaline NH_3 electrolytic cell decomposes the liquid NH_3 and produces H_2 in the proposed system. The main electricity source of the electrolysis is the solar energy system in the PV/PEMFC design. Excessive solar power is used in the CI operation or sold to the grid depending on the operational load. The investigated system has been benchmarked with a PV/Battery system, and onboard electricity generation options environmentally and economically. The PV/Battery system provides the electricity directly to the ships. As the onboard marine diesel generator options, the conventional systems using light fuel oil (LFO) and dual-fuel engines utilising LNG have been assessed. When there is not enough electricity to meet demand, the national grid connection supports both CI alternatives. The comparison also assesses the use of the national grid for electricity alone. The innovative component of this work is the evaluation and benchmarking of all feasible possibilities considering onshore H_2 production using solar power and grey, blue, and green NH_3.

To perform the analysis, the monthly arrival and departure data including vessel electrical needs have been taken from a reference port in Kocaeli, Türkiye. The fuel consumption and emissions of onboard electricity production plants have been calculated for the port in a month. The integration of PV/PEMFC and PV/Battery systems has been modelled in Python and their environmental and economic parameters have been calculated. Upstream and operational GHGs have been expressed by calculating equivalent carbon dioxide (CO_{2e}) and the economic performance has been measured by the LCOE and payback period (PBP).

2. METHOD

This section explains the system properties used in analyses and the mathematical background of the calculations. Figure 1 illustrates the flowchart of methods used in the study.

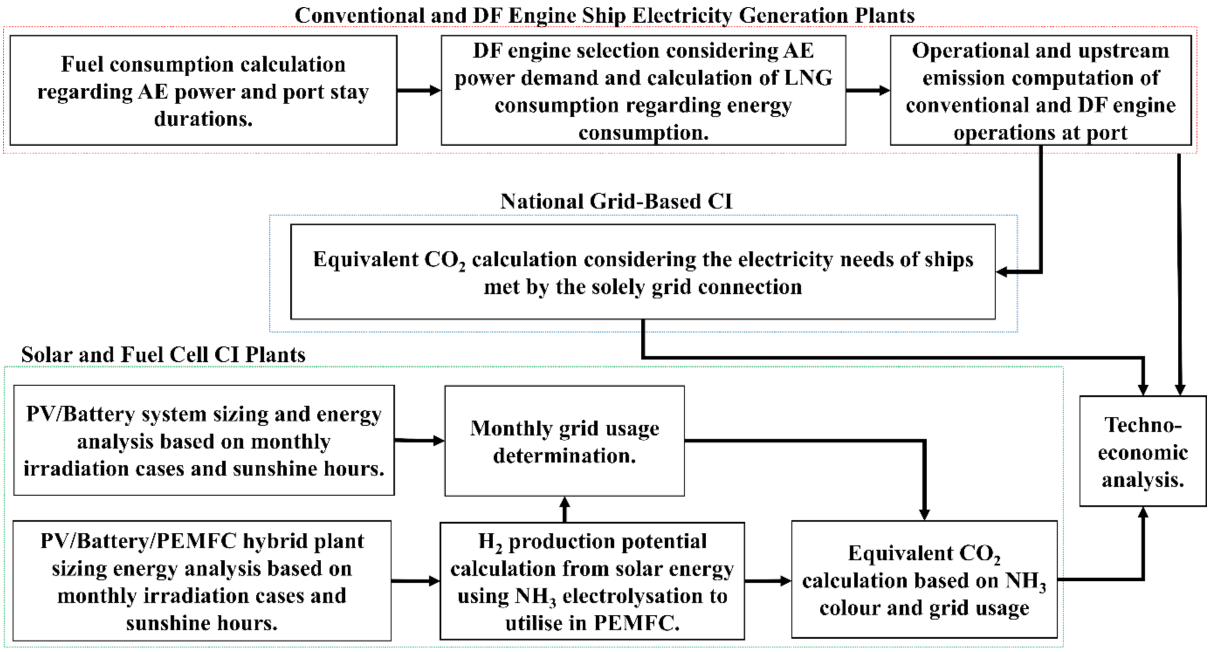

Figure 1. Method flowchart.

To determine the CI options and their environmental and economic prospects, the monthly data containing operation times and diesel generator properties of ships have been collected in a port facility. Using the data, marine vessels' fuel consumption has been calculated for conventional marine diesel engines (MDEs) at port operation. Regarding the diesel engines' power output, possible dual fuel (DF) engines have been selected for each vessel. Assuming ships use LNG at port, the fuel consumption of the DF engine operations has been calculated. Operational/upstream GHG emissions and resulting CO_{2e} from conventional and DF engines have been calculated. In addition, CO_{2e} resulting from the shore connection using the grid has been calculated for the comparison.

Two renewable-energy-based plant (RE plant) designs are presented in the study. The first one involves only PV cells and batteries. The electricity generated from the sun during the day charges batteries which ensures shore connection to the vessels at night. The PV panels also directly provide energy to the vessels in the daytime. When solar power does not meet the operational demand, the grid electricity connection is used for CI operation.

The second plant design consists of PV panels, batteries and PEMFCs when the energy demand is too large, the grid energy has been kept usable. The required monthly H_2 has been calculated and a part of the energy produced in PV Panels has been utilised to generate H_2 through NH_3 electrolysation. This design aims to obtain the highest CO_{2e} reduction in emissions resulting from the port operations of the ships. The CO_{2e} of the RE plant has also been computed and all options for CI have been compared environmentally. Finally, a cost-benefit analysis has been conducted to evaluate whether RE plants are feasible investments and to discuss the tariff for these services.

2.1. System Properties

The data collected from the port facility involve arrival-departure times, main engine (ME) properties and auxiliary engine (AE) powers. Figure 2 illustrates the gross tonnage (GT), length overall (LOA) and ME/AE powers of the ships that arrived at the case study port in a month.

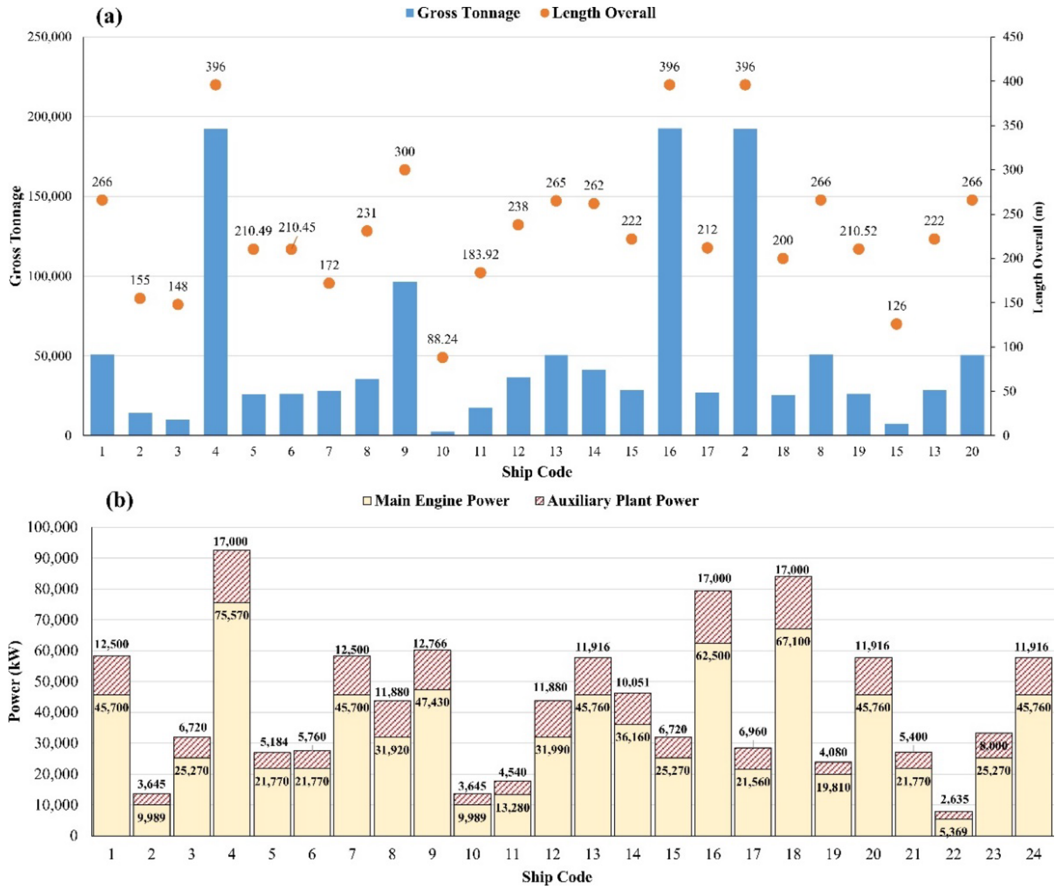

Figure 2. The GT/LOA (a) and AE/ME power (b) distributions of the ships.

In the case study, 24 vessels made a total of 31 arrivals and departures within a month. Of these, 23 were container carriers, and one was a general cargo vessel. The largest vessel had an LOA of 396 meters and a GT of 192,784, while the smallest had an LOA of 88.94 meters and a GT of 2,451. The average LOA across all vessels was 235.11 meters, with a mean GT of 52,410.6 as shown in Figure 2 (a). The AE power outputs have ranged from 2,635 to 17,000 kW, while the ME powers have varied between 5,639 and 75,570 kW demonstrated in Figure 2 (b). The average power outputs for the ME and AE have been 33,436.13 kW and 9,233.88 kW, respectively. The port staying times in days and the required AE energy during the port operations of each arrival are illustrated in Figure 3.

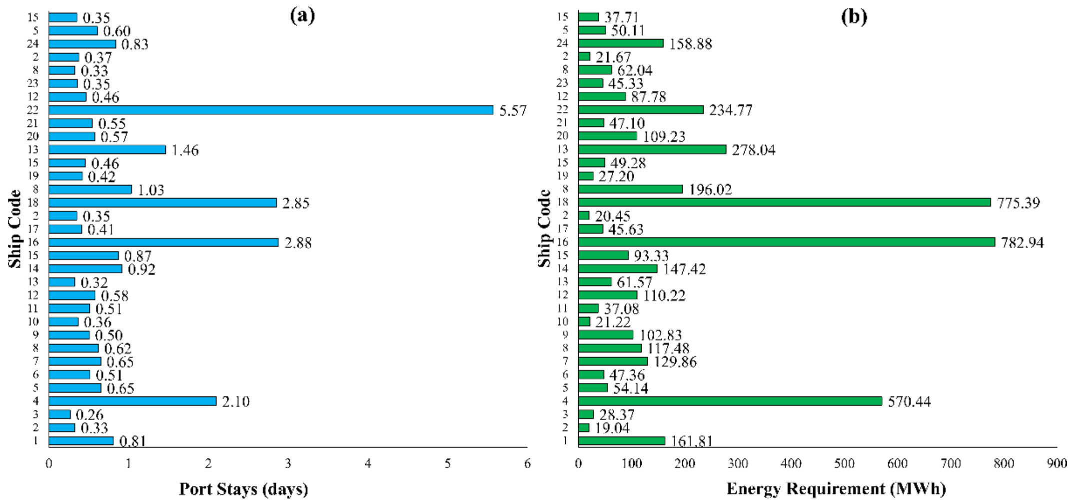

Figure 3. The port stays durations (a) and the required AE energy (b) of the ships.

The total monthly energy requirement for the vessels has been 2,933.68 MWh. The average capacity of marine electricity generation plants has been 8.942 MW, and vessels have stayed in port for an average of 1 day. The longest and shortest port stays have been 5.57 and 0.26 days, respectively, as depicted in Figure 3(a). The largest energy requirement has been 782.94 MWh, while the smallest has been 19.04 MWh as shown in Figure 3 (b). Specific fuel consumption (SFC) of the conventional and DF engines has been collected from Wärtsilä (2024). The calculations for diesel engines have been conducted regarding LFO while LNG is assumed to be used in DF engines. Figure 4 indicates the AE SFC values of the diesel and DF plants for the evaluated ships that stayed in the port.

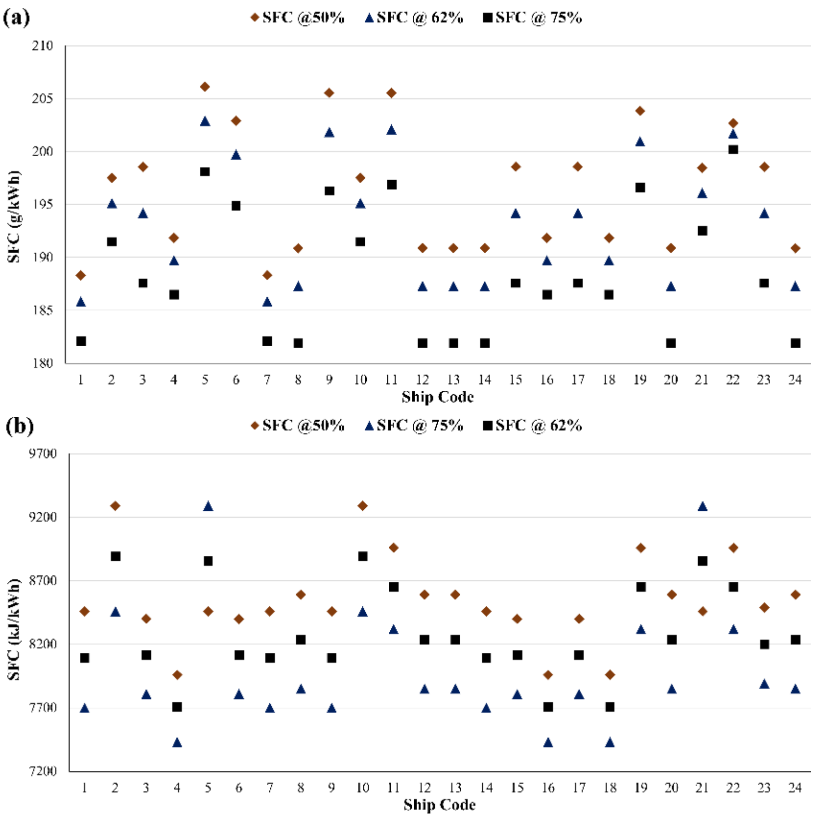

Figure 4. LFO SFC (a) and LNG specific energy consumption (b) regarding 50, 62, and 75% generator loads (Wärtsilä, 2024).

The SFC of marine diesel generators has been taken at 62%, interpolated from the 50% and 75% load data. The mean-variance of SFC and LNG energy consumption has been 0.4%, which has been lower compared to other uncertainties. The properties of PV panels, batteries and PEMFCs have been demonstrated in Table 1.

Table 1. Hybrid electricity supply plant specifications (JNGE, 2022; Panasonic, 2022; PowerCellGroup, 2024; SMA, 2021; TommaTech, 2023)

	PV Panels	
Parameter	Value	Unit
Maximum Power	460	W
Efficiency (η)	21.13%	-
Maximum Voltage	41.8	V
Maximum Current	11	A
Temperature Range	-40/+85	ºC
Weight	24.5	kg
Dimensions	2095 x 1039 x 40	mm
	Battery	
Parameter	Value	Unit
Capacity	3.45 (typical), 3.35 (minimum)	Ah
Chemistry	Lithium-ion	-

Charging Method	CC-CV	-
Typical Charging Current	1.475	Ah
Typical Charging Time	270	min
Gravimetric Energy Density	224	Wh/kg
Nominal Voltage	3.6	V
Length/Width/Diameter	65/18.5/9	mm
	PEMFC	
Parameter	Value	Unit
Power	200	kW
Gross Output DC Voltage	580	V
Gross Output Current	400	A
Electrical Efficiency (Peak)	54%	-
Fuel Consumption	98.4	Nm3/h
Heat Grade	<320	kW
Fuel Quality	Pure H_2 ISO 14687:2019	-
Length/Width/Height	730/900/2200	mm
	Inverter	
Parameter	Value	Unit
DC Voltage Range	634-1000	V
Maximum DC	3960	A
Maximum AC Power	2475	kVA
Efficiency	98.6%	-
System AC Voltage	440	V
	Maximum Power Point Tracker (MPPT)	
Parameter	Value	Unit
PV Max Input Voltage	480-800	V
PV Max Input Current	50-100	A
PV Max Input Power	1.2-58.4	kW

The capacity of the PEMFC system in the PV/PEMFC configuration has been determined based on the maximum load demand of berthed ships at the port. The port operates one ship at a time, with the peak power demand recorded at 2,782.56 kW when two generators are utilised at up to 62% load. Under these conditions, the average power demand has been calculated as 3,593.08 kW. Based on this analysis, a configuration involving 17 PEMFC units has been selected for the PV/PEMFC system. In this configuration, battery packs are integrated as a safety device having a capacity of 1,700 kWh (half of PEMFC power can be met by batteries for an hour) to provide quick response during sudden load changes, compensating for the operational loads. This complements the PEMFCs, which are primarily responsible for meeting the stable electrical load requirements (Korkmaz et al., 2023; Yuksel, 2023). The capacity of the PV panels has been determined based on the required H_2 to operate the PEMFCs in worst-case scenarios of irradiation and sunshine hours (the month of December minimum irradiation data). A total of 3,353 PV panels have been assumed to be installed, covering an area of 7,297 m².

In the PV/Battery configuration, the same number of PV panels and equivalent area have been utilised while the battery capacity has been determined based on the charging capacity of the panels. In the worst-case scenario, the batteries are required to charge during daylight hours. To ensure maximum battery lifespan and stable operation, the state of charge has been maintained between 20% and 80% (Saxena et al., 2016). Based on these considerations, the battery capacity has been set at 13,199.80 kWh. Inverter and MPPT numbers have been adjusted considering their maximum input values and used two sets of each equipment to distribute the power. Figure 5 illustrates the general system layouts of the investigated shore-based RE Plants.

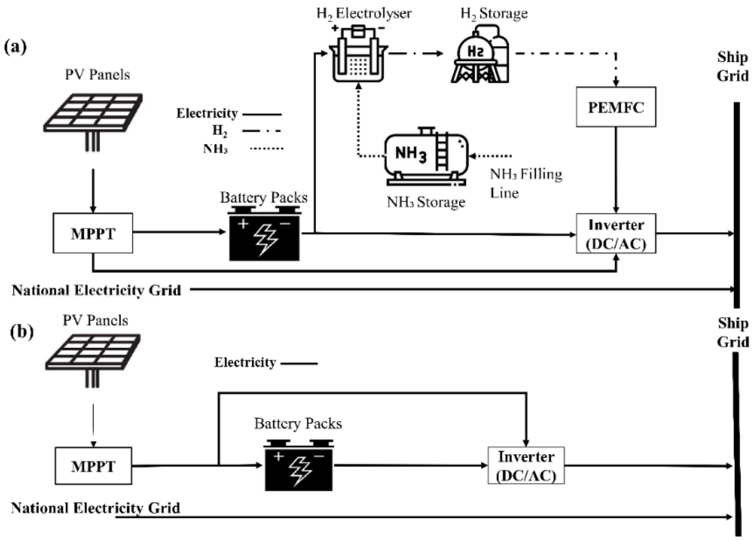

Figure 5. System layout of the RE Plant: (a) PV /PEMFC, (b) PV/Battery.

In the PV/PEMFC system, the PV panels directly support the grid after fulfilling the demand of the electrolyzer. Additionally, they are connected to charge the batteries, if the batteries are utilised in an instant load demand. During the day, solar-generated electricity charges batteries, ensuring a shore connection to vessels at night in the PV/Battery RE plant. Additionally, PV panels directly supply energy to the vessels during daylight hours. If solar power is insufficient to meet operational demands, grid electricity undertakes the operation.

The preference for using NH_3 over seawater in the PV /PEMFC plant is based on energy requirements, as seawater electrolysis necessitates a higher energy input (Atchison, 2021). The NH_3 electrolyser requires 1.55 kWh per 1 kg H_2 production and 1 kg NH_3 produces 0.17 kg H_2 (Babar & Botte, 2024; Boggs & Botte, 2009; Rivarolo et al., 2019). On the other hand, seawater electrolysis can require up to 55 kWh per 1 kg H_2 (Atchison, 2021). The electrolyser capacity has been determined based on the calculation of monthly energy demand, assuming an energy consumption of 1.55 kWh per 1 kg of H_2 produced. Considering the 3,400-kW capacity of the PEMFC, the required electrolyser capacity has been calculated at 170.75 kW.

Considering the NH_3 generation potential of the region, the NH_3 decomposition based on solar energy has been selected for the H_2 production methodology (GovUK, 2022; IGSAS, 2022). Using an alkaline electrolytic cell the process of NH_3 decomposition to produce high-purity H_2 is defined in Equations 1 to 3 (Little et al., 2015; Vitse et al., 2005). The choice of an alkaline electrolyser has been influenced by its commercial availability, technological maturity, and lower costs compared to PEM and solid oxide electrolysers (Kim et al., 2022; Nami et al., 2024; Rouwenhorst, 2023).

$$Anode: 2NH_3(aq) + 6OH^- \rightarrow \; N_2\,(g) + 6H_2O + 6e^- \tag{1}$$

$$Cathode: 6H_2O + 6e^- \rightarrow \; N_2\,(g) + 3H_2 + 6OH^- \tag{2}$$

$$Overall\ Reaction: 2NH_3(aq) \rightarrow \; N_2\,(g) + 3H_2(g) \tag{3}$$

The synthesis of NH_3, primarily through the Haber–Bosch process, is one of the largest industrial operations globally. Consequently, the infrastructure for its storage and transport is well-established. Unlike H_2, NH_3 can be easily liquefied at pressures below 10 bar, achieving an energy density of 13.6 GJ m^{-3} (Little et al., 2015). With a thermodynamic voltage of 0.1 V, NH_3 decomposition generates H_2 that can be used in H_2 FCs. This interconversion between H_2 and NH_3 offers a potentially more efficient method for H_2 storage and transport compared to direct H_2 compression (Hanada et al., 2010; Little et al., 2015; Nami et al., 2024; Vitse et al., 2005).

The PV panels controlled by an MPPT generate and send energy to battery packs. Determined battery capacity is used to assist H_2 production and meet the electricity demand of vessels daily. Part of some energy is used in the H_2 production and sent to the PEMFC to produce stable electricity while depending on the month excess power is supplied to the grid of ships. Figure 6 illustrates the minimum, average and maximum global horizontal irradiance (GHI) values denoted as irradiation in the port location where the port in the case study is located.

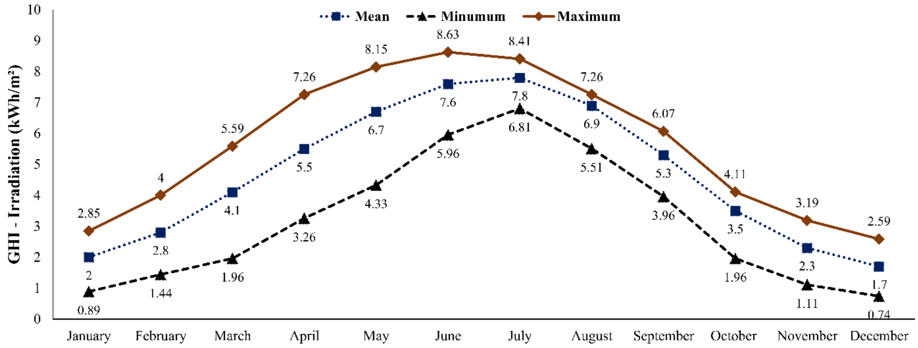

Figure 6. Minimum, average and maximum irradiation values regarding months in port location (WeatherSpark, 2024).

The lowest, medium, and highest irradiation values in the specified region have been indicated. The variations have been utilised in the uncertainty analysis to determine whether a scenario-based approach is necessary for the parameter. The largest deficit is in May where the difference in the lowest and average values have reached 2.37 kWh/m^2. The gap is smallest in July with a mean variation rate of around 10%. A similar case has been valid for sunset-sunrise times and resulting hours of sunshine through months. Figure 7 indicates minimum, average, and maximum sunset/sunrise times and regarding hours of sun are indicated in Figure 8.

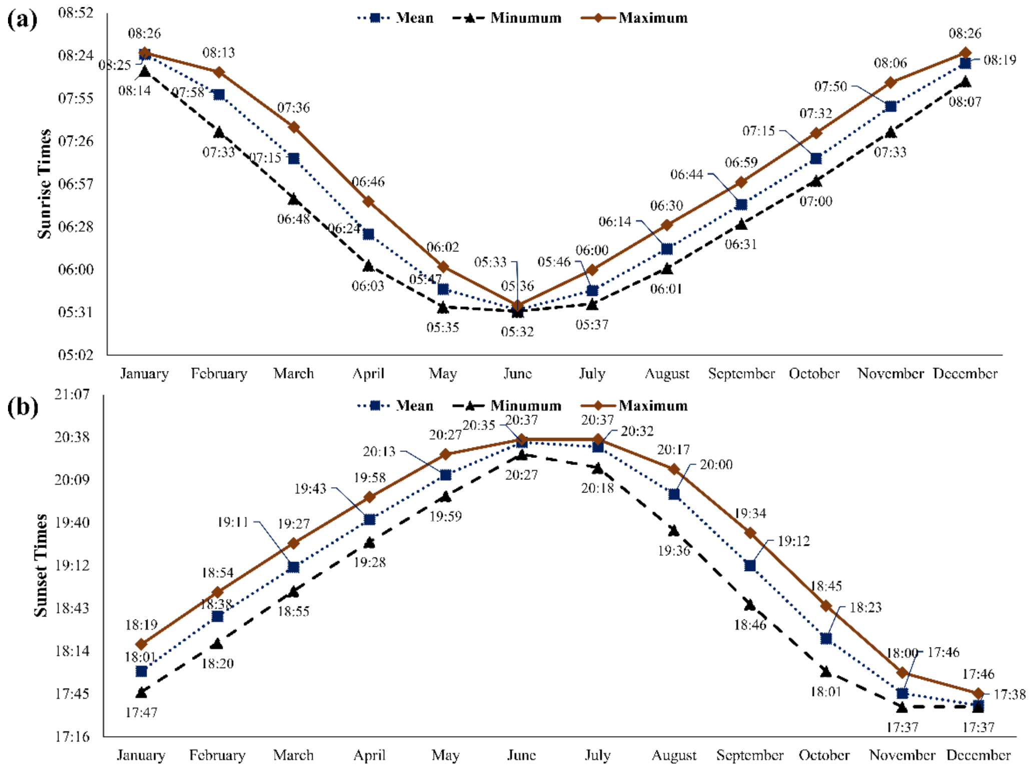

Figure 7. Minimum, average and maximum sunrise (a) and sunset (b) regarding months in port location (WeatherSpark, 2024).

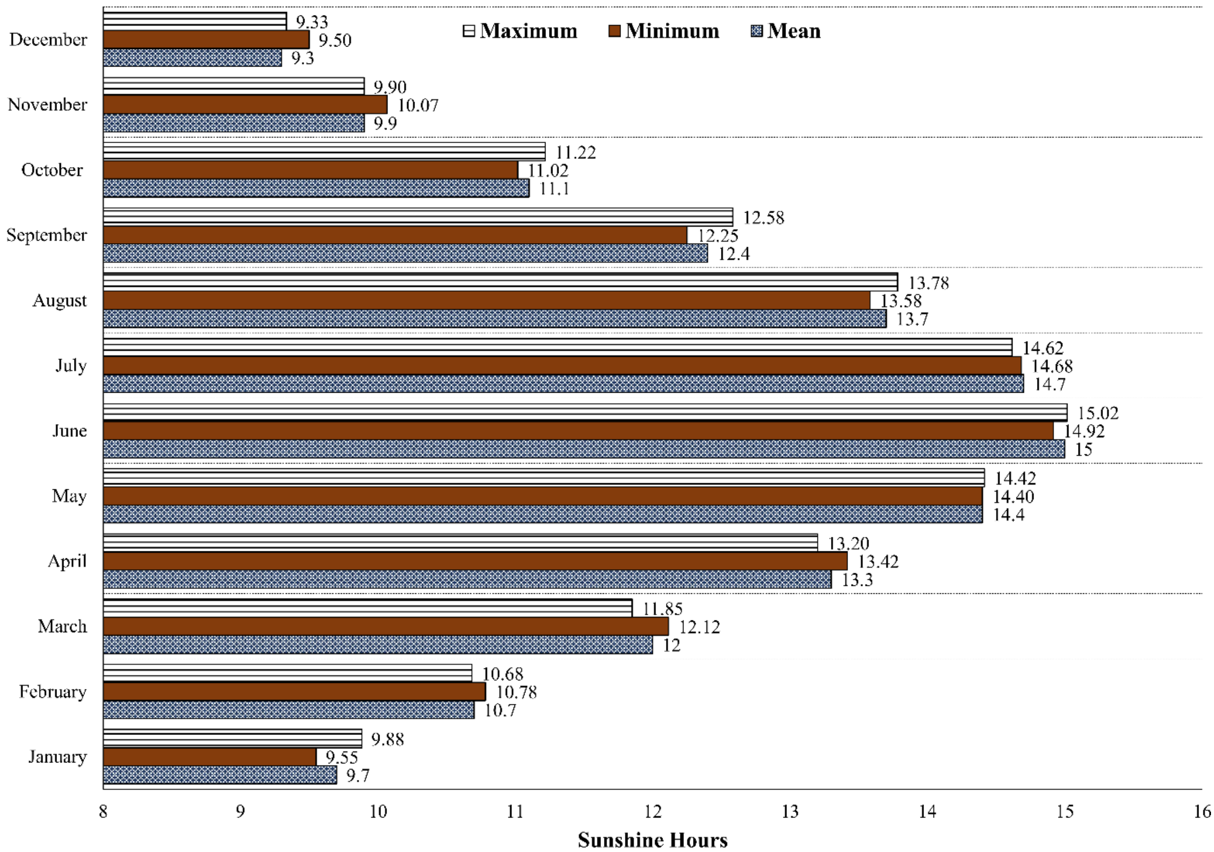

Figure 8. Minimum, average and maximum hours of sun regarding months in port location (WeatherSpark, 2024).

The trend in irradiation has been valid for sunrise, sunsets, and sun hours however, the rate variations have been much lower than the irradiation. By utilising daily sunshine hours, along with sunset and sunrise times, the day and night operation durations have been calculated based on the vessels' arrival and departure schedules. The operational energy demands have been compared with the monthly available energy from the solar plants to assess the necessity of grid power and identify any surplus solar energy. The total day and night operation durations have been estimated, assuming the ship and port stay patterns remain consistent across other months. In the PV/Battery configuration, solar panels have supplied energy to vessels either through battery storage or directly, whereas in the PV/PEMFC design, they have been used to generate H_2 for the PEMFC system. The required H_2 of the PEMFCs have been calculated by utilising curves provided by the manufacturer shown in Figure 9 (PowerCellGroup, 2024).

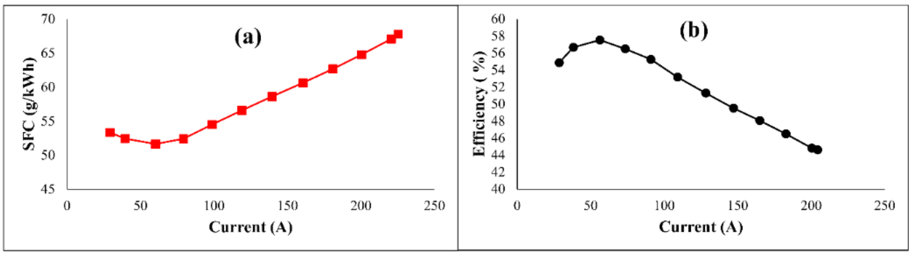

Figure 9. SFC-Current (a) and Efficiency–Current (b) curves of the PEMFC stack (PowerCellGroup, 2024).

Regarding the operational load demand of the vessels, the required power and current of PEMFCs have been calculated. The load has been assumed to be equally distributed between stacks and SFC of the each PEMFC has been interpolated from the curve given in Figure 6 (a). Using a degradation rate of 0.5% per 1000h (Fang et al., 2019; Yuksel, 2023; Zarabi Golkhatmi et al., 2022) the efficiency drop at the matching current has been employed to the SFC value increasing SFC.

2.2. Mathematical and Logical Background

The fuel consumption of internal combustion engines in the analysis has been conducted by employing Equation 4 (Bayraktar et al., 2023).

$$Fuel\ Consumption\ (g) = SFC\ \left(\frac{g}{kWh}\right) x\ P\ (kW) x\ t_{op}(h)\ x\ NoG \tag{4}$$

where P is the power of one generator, t_{op} is the operation time and NoG is the number of working generators. P is calculated for each ship according to the size of marine electricity generation plants and assuming three generators in the plant. At the port, two generators were assumed to work at up to 62% (evaluated between 50% and 75% SFC variance) load (Yuksel & Koseoglu, 2023; Yüksel & Köseoğlu, 2022). The H_2 consumption of PEMFCs has been computed by using Equation 5 (Lan et al., 2022; Yuksel, 2023).

$$\mathrm{H}_2\ Consumption\ (g) = t_{op}(h)\ x\ P_{PEMFC}(kW)\ x\ \ SFC_{PEMFC} \tag{5}$$

The PEMFC power (P_{PEMFC}) and SFC have been determined by using Figure 6 Equation 6 indicates the computation of the energy output of one PV panel (E) (Aijjou et al., 2019; Gülmez et al., 2024).

$$E\ (kW) = A_P(m^2)\ x\ \eta\ x\ \ H_a\ (kWh/m^2) x\ P_r \tag{6}$$

A_P is the one solar panel area, η is 21.13%, and P_r represents the performance ratio, which indicates how efficiently a solar photovoltaic system converts sunlight into electricity. However, the specific performance target can vary based on factors like geographic location, system design, and technology. A typical value for P_r is between 0.75 and 0.80 and taken at 0.75 in this study (Urrejola et al., 2016). H_a is the mean solar irradiation shown in Figure 6. The energy demand of the vessels (E_d) has been formulated in Equation 7. (Yüksel et al., 2024).

$$E_d(kWh) = P(kW)\ x\ \ t_{op}\ (h) x\ 2\ x\ 0.62 \tag{7}$$

Two generators up to 62% load have been assumed to work during the port operations. The PEMFC capacity has been determined to meet the maximum energy and power demand. The capacity of the PV panels has been calculated using Equation 8 (Babar & Botte, 2024).

$$Required\ Panel\ Capacity\ (kWh) = \frac{Dailiy\ H_2\ Consumption\ (kg)}{1.55\ (\frac{kWh}{kg})} \tag{8}$$

The number of required panels has been calculated based on the minimum sunlight hours and irradiation conditions. The calculation process is outlined in Equation 9. The required panel area has been computed by employing Equation 10 (Gülmez et al., 2024).

$$Required\ Panel\ Number\ \ = \frac{Required\ Panel\ Capacity\ (kWh)}{E\ (kW)\ @\ minumum\ \ H_a\ and\ sun\ hours} \tag{9}$$

$$Required\ Panel\ Area(m^2) = Required\ Panel\ Number * A_P \tag{10}$$

The battery capacity in the PV/Battery system has been selected based on the available charging hours by employing Equation 11. Using the required panel capacity and considering the minimum H_a and sunlight hour conditions, the batteries are required to charge during the day.

$$Battery\ Capacity(kWh) = Available\ Charging\ Hours * E *\ Required\ Panel\ Number \tag{11}$$

The calculations described above have been ensured with a Python simulation iteratively for each vessel demand and varying months of the year. The algorithm scheme which explains the logic of this simulation is illustrated in Figure 10.

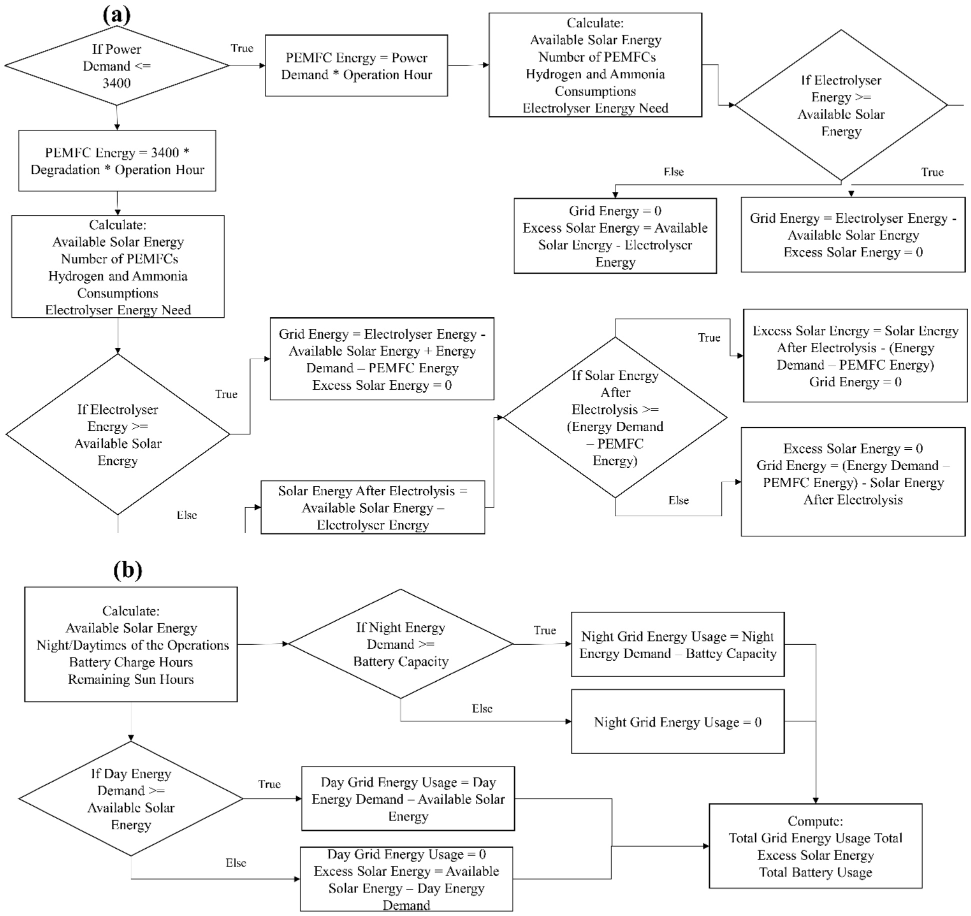

Figure 10. The algorithm scheme of (a) PV/PEMFC and (b) PV/Battery system simulations.

In the PV/PEMFC system model presented in Figure 10(a), the process begins by assessing the power demand, which triggers the system. The energy allocation for the PEMFC is determined based on the results. After calculating both the energy consumption and solar energy capacity, the system ensures whether the solar energy can meet the electrolyser demand. Depending on the outcome, the required grid energy and any excess solar energy are subsequently determined.

In the PV/Battery configuration simulation depicted in Figure 10(b), the first step involves calculating the available solar energy, battery charging hours, remaining charge hours, and distinguishing between day and night operations based on the recorded arrival and departure times. The grid usage and excess solar energy are computed for various operational scenarios and months. Finally, the day and night calculations are consolidated to yield the total energy values. Based on the total H_2 and NH_3 consumptions environmental and economic analyses have been performed.

The environmental analysis has been conducted by considering upstream and operational GHG emissions including GHGs and other emissions including NO_x, SO_x, PM, and volatile organic compound (VOC)by using operational (C_o) and upstream (C_u) coefficients in Table 2 (Gilbert et al., 2018; Kuittinen et al., 2023; Kuzu et al., 2021; Yuksel, 2023; Yuksel et al., 2024).

Table 2. Coefficients for upstream and operational GHG emissions (g-C_u/g-C_o).

Co	CO_2	N_2O	CH_4	**NO_x**	**SO_x**	**PM**	**VOC**
LFO	3.114	0.00015	0.00006	0.090	0.025	0.0028	0.0031
LNG	2.75	0.016*	3.5124*	1.170*	0.003*	0.027	0

C_u	CO_2	N_2O	CH_4	NO_x	SO_x	PM	VOC
LFO	0.1481	0	0.36*	0.016	0.102	0.028	0
LNG	0.1304	0	1.0799*	0.111	0.771*	0	0

*The unit is g/kWh

Depending on the coefficient unit, the emissions have been calculated by multiplying coefficients with energy or fuel consumption. The starred coefficients have the unit of g/kWh and others have the unit g-emission/g-fuel in Table 2. Equation 12 calculates the CO_{2e} for the LNG and LFO scenarios (IMO, 2023).

$$CO_{2e}(t) = CO_2 + 265\ x\ N_2O + 28\ x\ CH_4 \tag{12}$$

The CO_{2e} is 0.4261 for grid electricity kg/kWh (CarbonFootPrint, 2023), 0.15 0 kg-CO_2/ kg-NH_3 for blue NH_3, 1.7 0 kg-CO_2/ kg-NH_3 for grey NH_3 when the feedstock is LNG and 0 kg-CO_2/ kg-NH_3 for green NH_3 (Hatzell, 2024). The LCOE is one of the primary methods used to evaluate the unit costs associated with various baseload technologies over their entire operational lifespan at the plant level (IEA, 2020), and has determined the economic feasibility of the evaluated systems. Equation 13 depicts the calculation of LCOE (Hansen, 2019; Taner & Sivrioglu, 2017).

$$LCOE\left(\frac{\$}{MWh}\right) = \frac{\sum_{t=1}^{n} \frac{(C_{plant}+C_{fuel}+C_{o\&m})\ (\$)}{(1+r)^t}}{\sum_{t=1}^{n} \frac{P_{gen}\ (kW) x\ t_{op}(h))}{(1+r)^t}} \tag{13}$$

where C_{plant} is the total investment cost during the installation, $C_{O\&M}$ is the operation and maintenance expenses, and C_{fuel} represents the fuel prices. The total generated power (P_{gen}) has been computed using the data, the lifespan of the system (t) has been taken as 20 years and the discount rate (r) has been assumed at 7% (IEA, 2020; Shu et al., 2017). Table 3 demonstrates the C_{plant}, $C_{O\&M}$ and C_{fuel}. The investment costs, originally sourced from older references, have been updated using the Chemical Engineering Plant Cost Index (CEPCI), which stands at 800.3 for May 2024 (latest official announcement) ((Maxwell, 2024). The investment costs have been adjusted by multiplying the original values by the ratio of the recent CEPCI value to the respective year's CEPCI, ensuring an accurate price update. (Konur et al., 2022).

Table 3. The fuel, installation, and operation costs.

Equipment	C_{plant}	$C_{O\&M}$	Unit	Reference
PV Panel	358	1%	$/unit	(TommaTech, 2023; Yüksel et al., 2024)
Battery	11.82	1%	$/cell	(Yüksel et al., 2024; Yuksel & Koseoglu, 2023)
PEMFC	2,540.46	1.5%	$/kW	(Wang et al., 2022)
H_2 Storage	492.2	1%	$/kg	(Terlouw et al., 2022)
H_2 P&T	2440	4%	$/kW	
NH_3 P&T and Storage	3,145,236	31,083	$	(Seo & Han, 2021)
Electrolyser	251.54	2%	$/kW	(Kim et al., 2022; Rouwenhorst, 2023)
Balance of System	48.15	2%	$/kW	(Terlouw et al., 2022)
MPPT	5.59	1%	$/A	(JNGE, 2022)
Inverter/Transformer	553.84	1%	$/kW	(El-Khozondar et al., 2022)
CI Infrastructure	8,875,726	443,786	$	(Innes & Monios, 2018)
HFO Storage	1497.3	1%	$/m³	(Ammar & Seddiek, 2023)
LNG Storage	3800	1%	$/kW	
MDE	240	1.5%	$/kW	
DF	387	1.5%	$/kW	

Fuel	C_{fuel} -Low	C_{fuel} -Medium	C_{fuel} -High	Unit	Reference
Grey NH_3	445	440	450	$/t	(Edwardes-Evans et al., 2024)
Blue NH_3	639.5	564	715.93	$/t	(Burges, 2024)
Green NH_3	775	700	1400	$/t	(Colak et al., 2021)
LFO	656	609	689	$/t	(ShipandBunker, 2024b)
LNG	680	570	797	$/t	
Carbon Price	76	94	112	$/t-$CO_2$	(ShipandBunker, 2024a)

$C_{O\&M}$ is calculated by multiplying the rates provided in Table 3 with the C_{plant}.The lifetime of PEMFC has been 40,000 hours (CORDIS, 2019). The battery lifespan has been taken as 5 years yielding 4 replacements of stacks (Yüksel et al., 2024). Storage equipment for NH_3 and H_2 has 20 years, and pressure and transfer (P&T) equipment and the balance of the system are assumed to last 10 and 7 years (Terlouw et al., 2022). Equation 14 indicates the calculation of PBP (Tian et al., 2021).

$$PBP\ (years) = \frac{C_{plant}}{C_{flow}} \tag{14}$$

where C_{flow} is the net cash flow calculated by the gain from the tariff minus expenses (Hazar et al., 2023). The grid electricity price in Turkiye is 0.16 $/kWh after adjusting with the exchange rate between the Turkish lira and the United States dollar (USD) on 10/07/2024 (Inanc, 2024). The excess solar energy during the operations is assumed to be sold to the provider at 133 $/MWh (Inal & Down, 2020).

2.3. Uncertainty Analysis

A critical concern is the accuracy of the measured or collected data and the results derived from analyses. Uncertainty serves as an indicator of the reliability or "goodness" of a result. In the absence of this measure, it becomes challenging to assess the suitability of the data as a foundation for informed decision-making in areas such as health, safety, commerce, or scientific rigour (Esen et al., 2007). The uncertainty analysis among the statistical approaches can effectively determine the scenarios based on uncertainties and ensure data accuracy (Taner & Sivrioglu, 2015). The combination of different uncertainty levels is calculated by employing Equation 15 (Taner, 2015).

$$U_R = \sqrt{\left[\left(\frac{\delta R}{\delta x_1}U_1\right)^2 + \left(\frac{\delta R}{\delta x_2}U_2\right)^2 + \cdots + \left(\frac{\delta R}{\delta x_n}U_n\right)^2\right]} \tag{15}$$

In Equation 10, U values represent the fractional uncertainties of each independent variable (x_1, x_2,…x_n) while the U_R is the uncertainty of the combined calculation. R depicts the result or used value for each independent parameter (Akpinar, 2006; Esen & Yuksel, 2013). Figure 11 indicates the uncertainty map that illustrates the relation between the independent parameters used in this analysis.

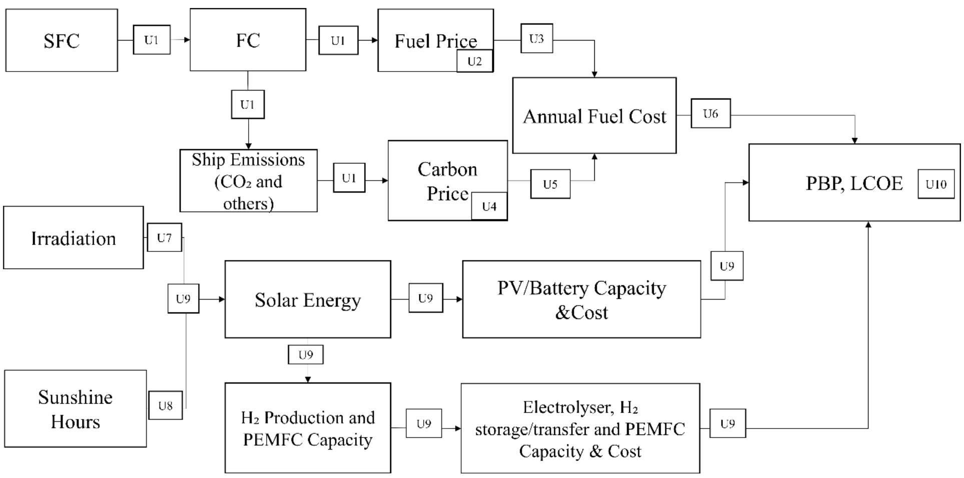

Figure 11. The uncertainty relationships of the analysis.

The uncertainty in SFC denoted as U1 introduces an error in the calculation of both fuel consumption and emissions. When combined with the uncertainties in fuel prices (U2) and carbon pricing (U4), U1 leads to the derived uncertainties U3 and U5, respectively. The total annual fuel cost uncertainty (U6) is then obtained by summing U3 and U5. Additionally, uncertainties are present in irradiation (U7) and sunshine hours (U8). By calculating the uncertainty of solar energy production (U9) using the multiplication uncertainty rule, the final total uncertainty in the economic analysis (U10) is derived from multiplying U9 and U6. The mathematical background of the calculation has been expressed in Equations 16 to 20 and the resulting uncertainties are illustrated in Table 4.

$$U_3 = \sqrt{[(U_1)^2 + (U_2)^2]} \tag{16}$$

$$U_5 = \sqrt{[(U_1)^2 + (U_4)^2]} \tag{17}$$

$$U_6 = \sqrt{[(U_3)^2 + (U_5)^2]} \tag{18}$$

$$U_9 = \sqrt{[(U_7)^2 + (U_8)^2]} \tag{19}$$

$$U_{10} = \sqrt{[(U_9)^2 + (U_6)^2]} \tag{20}$$

Table 4. Uncertainty analysis results.

U1	SFC	0.40%	U4	C_C	19.15%	U5	C_C + SFC	19.15%
	C_{fuel}			C_{fuel} + SFC			Annual C_{fuel}	
U2	VLSFO	6.10%	U3	VLSFO	6.11%	U6	VLSFO	20.10%
	LNG	16.69%		LNG	16.70%		LNG	25.41%
	Grey NH_3	1.12%		Grey NH_3	1.18%		Grey NH_3	19.19%
	Blue NH_3	11.88%		Blue NH_3	11.88%		Blue NH_3	22.54%
	Green NH_3	9.68%		Green NH_3	9.68%		Green NH_3	21.46%
Month	Irradiation	Sun Hours		VLSFO	LNG	Grey NH_3	Blue NH_3	Green NH_3
	U7	U8	U9	U10	U10	U10	U10	U10
January	49.00%	1.72%	49.03%	52.99%	55.22%	52.65%	53.96%	53.52%
February	45.71%	0.47%	45.72%	49.94%	52.30%	49.58%	50.97%	50.50%
March	44.27%	1.11%	44.28%	48.63%	51.05%	48.26%	49.69%	49.21%
April	36.36%	0.81%	36.37%	41.56%	44.37%	41.12%	42.79%	42.23%
May	28.51%	0.06%	28.51%	34.88%	38.19%	34.36%	36.34%	35.68%
June	17.57%	0.33%	17.57%	26.70%	30.89%	26.02%	28.58%	27.74%
July	10.26%	0.34%	10.26%	22.57%	27.40%	21.76%	24.77%	23.79%
August	12.68%	0.73%	12.70%	23.78%	28.41%	23.01%	25.87%	24.94%
September	19.91%	1.34%	19.95%	28.32%	32.30%	27.68%	30.10%	29.30%
October	30.71%	0.90%	30.73%	36.72%	39.87%	36.23%	38.11%	37.48%
November	45.22%	0.84%	45.23%	49.49%	51.87%	49.13%	50.53%	50.06%
December	54.41%	1.25%	54.43%	58.02%	60.06%	57.71%	58.91%	58.50%

The final uncertainty of the analysis has reached up to 60% when average values have been used, which falls outside acceptable limits. Irradiation and fuel prices have contributed the most to the overall uncertainty, leading to the adoption of a scenario-based approach to reduce the U10 value. By taking irradiation and fuel/carbon prices as a minimum, mean, and maximum, as shown in Figure 6 and Table 4, the overall uncertainty has become dependent on sunshine hours and SFC. Table 5 shows the U10 values after the uncertainties related to irradiation and fuel/carbon prices have been eliminated from the analysis.

Table 5. Uncertainty of scenario-based analysis.

January	February	March	April	May	June	July	August	September	October	November	December
1.76%	0.62%	1.18%	0.91%	0.40%	0.52%	0.53%	0.83%	1.40%	0.99%	0.93%	1.32%

The average uncertainty of the calculations has been reduced to 0.95%, with the highest value recorded at 1.40% in September and the lowest at 0.40% in May. The average values of SFC and sunshine hours, as shown in Figure 4 and Figures 7 and 8 respectively, have been used in the calculations. The monthly irradiation values have been categorised into minimum, average, and maximum, while fuel prices have been classified into low, medium, and high scenarios for the analysis. Equipment sizing, energy, and techno-economic analyses have been conducted based on this framework.

3. FINDINGS

The monthly LFO consumption of ships at berth has been found at 902.15 t yielding an annual 10,825.8 t. Considering ships have the same electric energy demand profile, the suitable DF engines for vessels have consumed 791.65 t of LNG leading to 9,499.8 t yearly. The operational and upstream GHG and other emissions in a year due to these consumptions are illustrated in Figure 12.

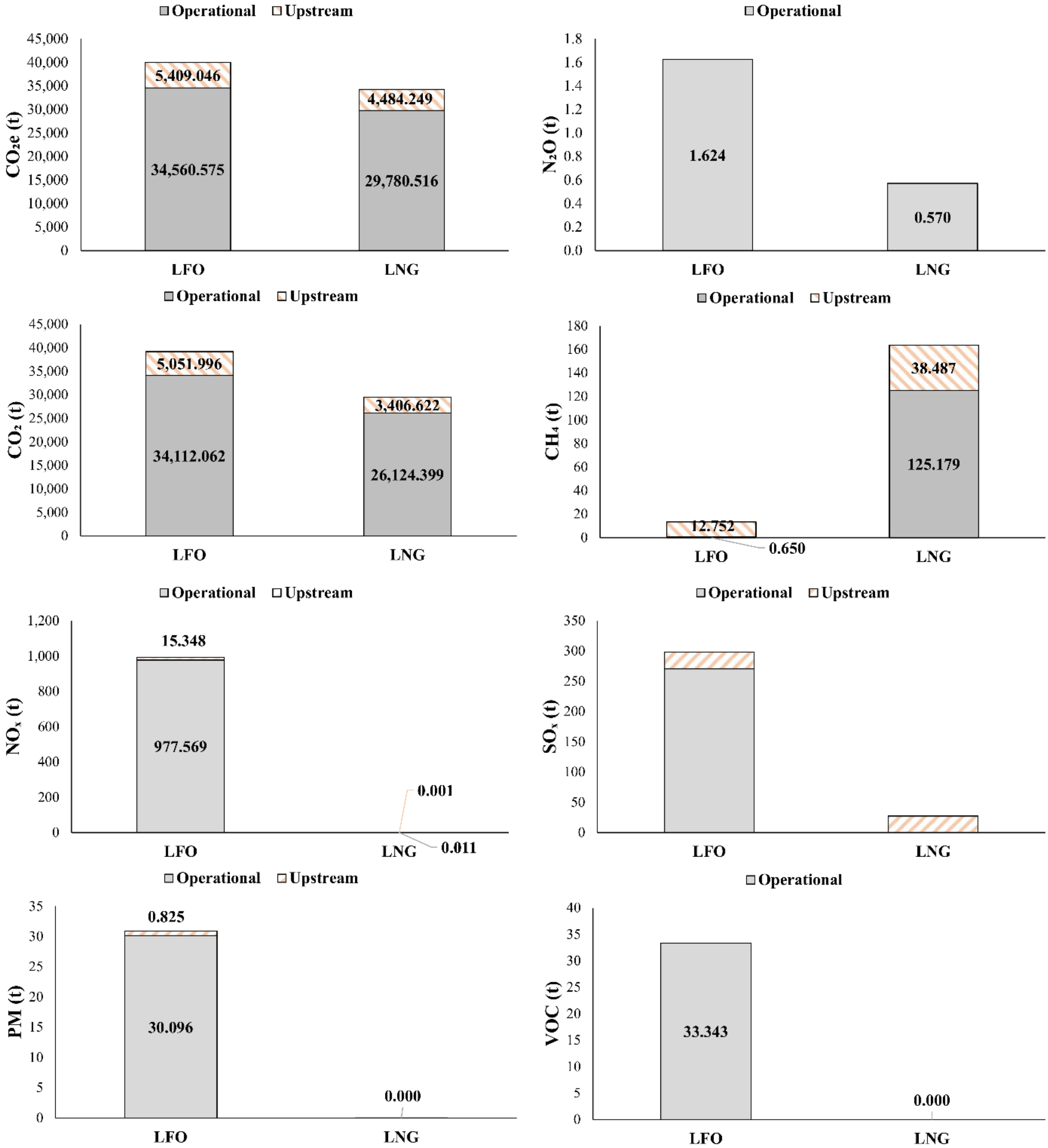

Figure 12. Monthly operational/upstream GHG and other emissions on board electricity generation scenarios.

The LNG utilisation has reduced the operational CO_2 by 23.42% resulting in a similar reduction ratio in upstream CO_2 emissions. The deduction of operational N_2O has been larger at 64.88% while operational and upstream CH_4 has skyrocketed. As the primary fuel on DF engines, LNG has decreased operational and upstream CO_{2e} by 13.83% and 17.1%, yielding 14.27% of total CO_{2e} deduction.

Annually, LFO plants have produced operational 977.57 t of NO_x, 270.65 t of SO_x, 30.1 t of PM, and 33.34 t of VOC. Operationally, the use of LNG has successfully eliminated these emissions, with the exception of SO_x emissions from upstream processes, which remain at levels comparable to those of LFO. Overall, NOx and PM emissions have been nearly eliminated, VOC emissions have been fully eliminated, and SOx emissions have been reduced by 90.79%. On the other hand, the usage of RE plants has eliminated non-GHG emissions. Figure 13 indicates the daily panel capacities in MW, the H_2

production capacity of the electrolyser regarding the solar capacity, and the produced/consumed H_2 for each berthed vessel.

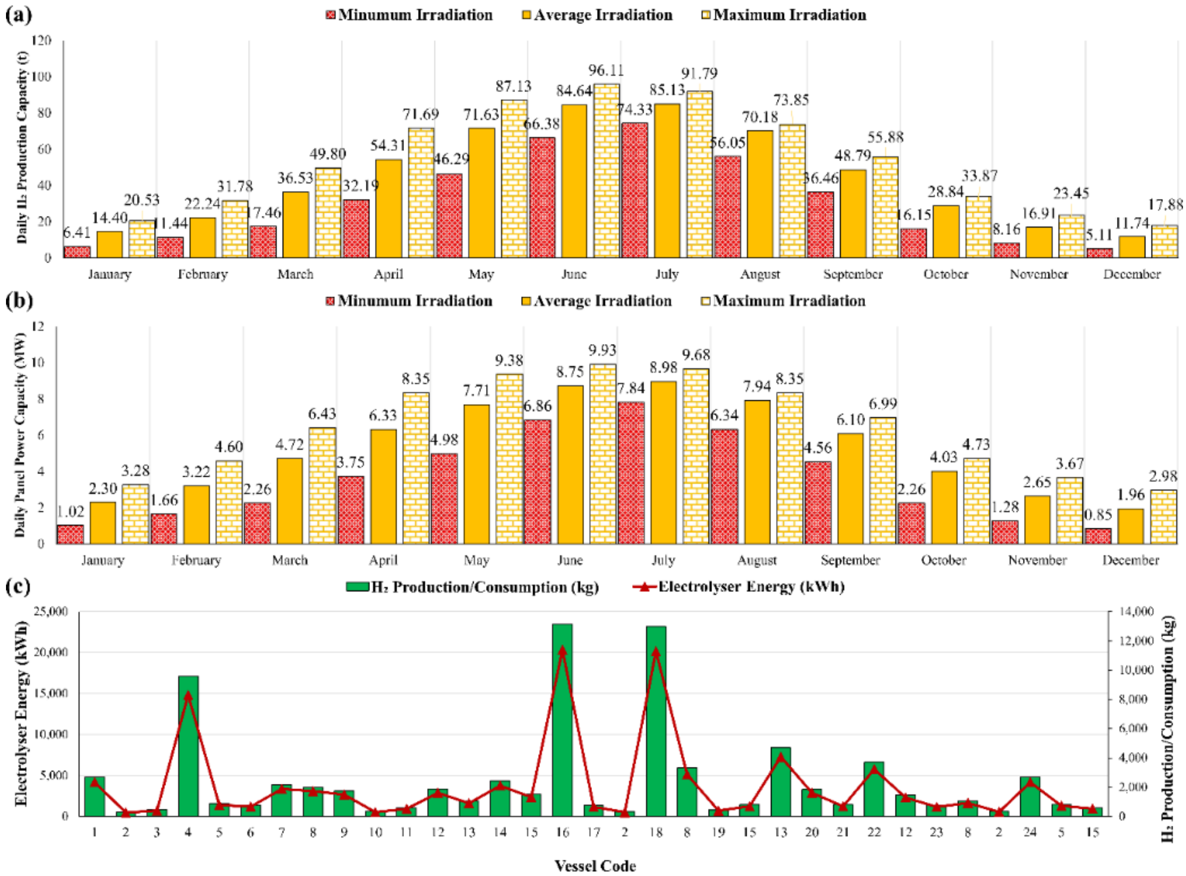

Figure 13. (a) Daily H_2 production, (b) daily solar panel power output capacities, and (c) the relationship between consumed and produced H_2 in comparison to the electrolyser's energy requirements.

The daily H_2 production capacity can be increased to 96.11 tons per day in June, when maximum solar irradiation is available, as shown in Figure 13(a). This peak production is achieved when the entire capacity of the solar panels is dedicated to H_2 generation. However, the PV energy requirements have been based on the lowest irradiation period, which occurs in December for the selected region. In this scenario, the panels generate 0.85 MW of power, as shown in Figure 13(b), allowing for 5.11 tons H_2 production per day. This output is sufficient to meet the demand for all 17 units of PEMFCs within a single day. The average H_2 utilisation in the PV/PEMFC configuration, according to the graph in Figure 13(c), has been calculated at 2.63 tons per day, amounting to 946.71 tons annually. The required NH_3 to produce the H_2 has been found at 5,568.88 tons per year. Figure 14 illustrates the grid energy consumption and the surplus solar energy sold back to the grid for the PV/PEMFC configuration.

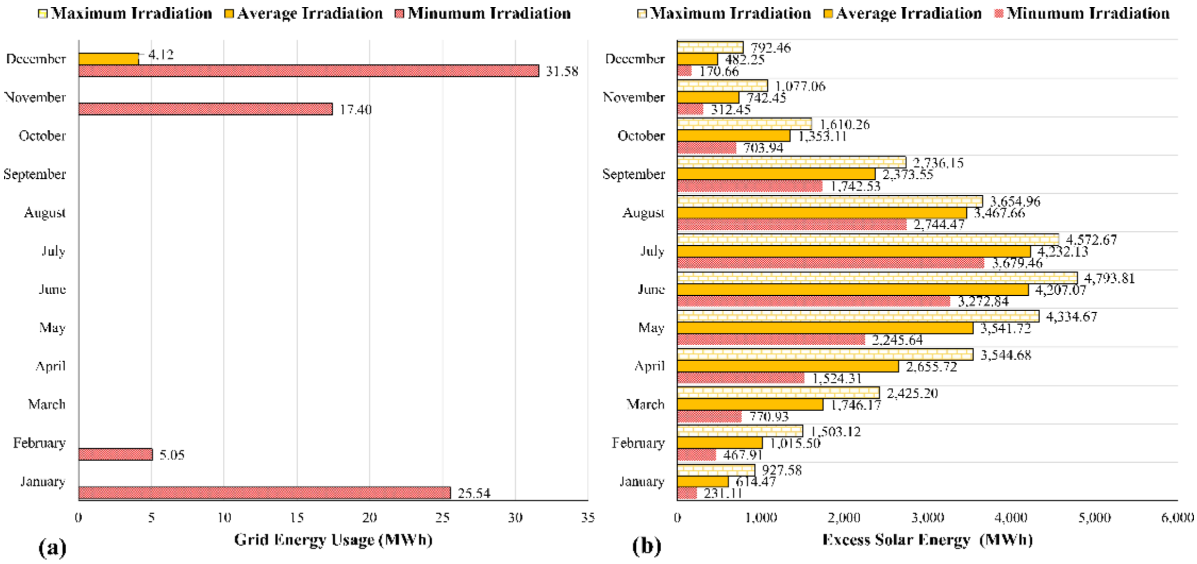

Figure 14. Grid energy usage (a), and excess solar energy (b) of the PV/PEMFC configuration.

The PV/PEMFC configuration does not require grid energy between March and October across all irradiation scenarios. Grid energy usage has varied from 4.12 to 31.58 MWh in December, depending on the irradiation levels shown in Figure 14(a). The annual grid energy usage has reached 79.58 MWh in the minimum irradiation case. Surplus solar energy has reached 4,793.81 MWh under maximum irradiation conditions. The lowest excess solar energy has been detected with minimum solar irradiation (in December) yielding 170.66 MWh, as illustrated in Figure 14(b). Figure 15 illustrates the total day-night operation time distribution according to months.

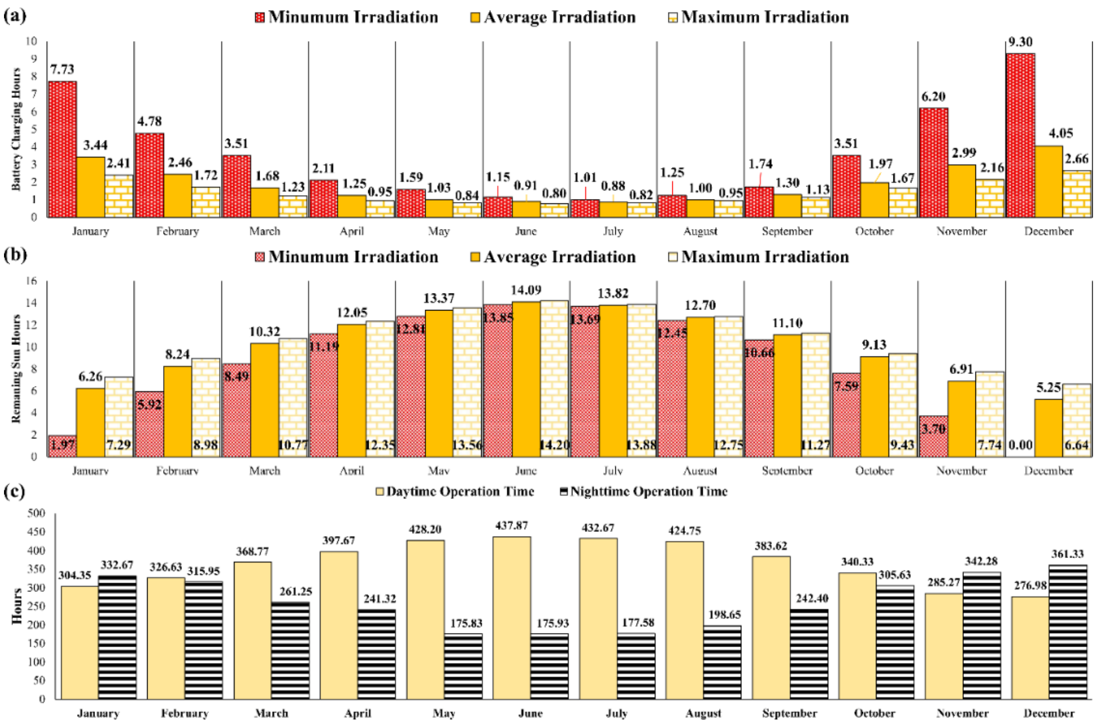

Figure 15. Battery charge hours (a), remaining sun hours (b), and total night/day operation hour distribution.

The battery charging hours, illustrated in Figure 15(a), have demonstrated nearly 1C charge rates, extending additional support from the PV panels to the CI operations, as indicated by the remaining sunlight hours in Figure 15(b). The longest charging times have been observed under the minimum irradiation scenario in December, with charge rates below 0.125 C-rate, followed by January, which exhibited similar irradiation levels, slightly exceeding 0.125 C-rate. The night and day operations in a month, shown in Figure 15(c), have been calculated based on vessel arrival/departure times and the corresponding sunrises and sunsets for each month. In June, the longest daylight operations have been recorded at 437.87 hours, while the longest dark operation hours, found in December, have reached 361.33 hours. Figure 16 demonstrates the required grid energy, surplus solar energy, solar energy supplied to the ships and night battery support of the PV/Battery configuration.

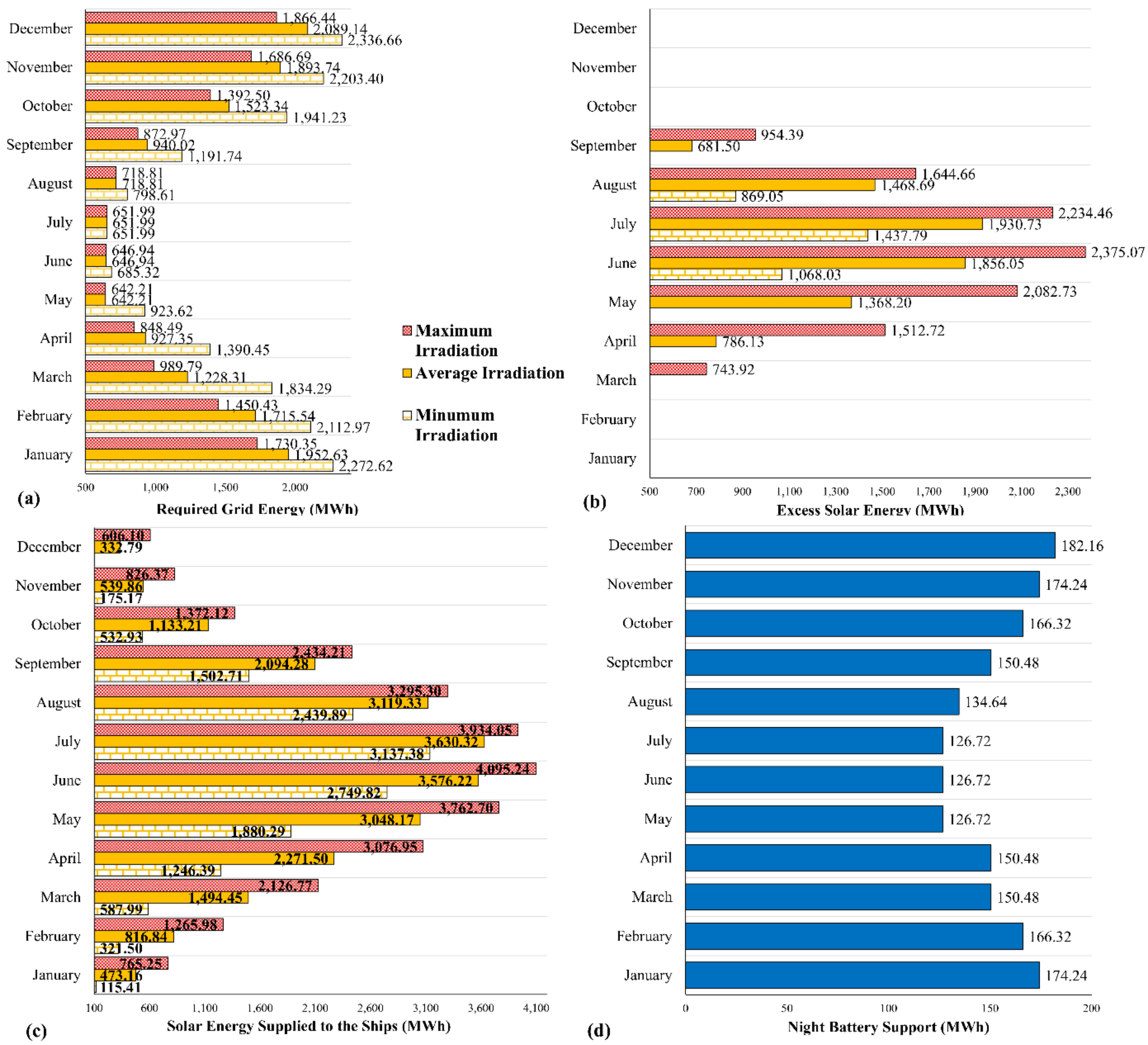

Figure 16. The required grid energy usage (a), excess solar energy (b), solar energy support to the ships (c), and night battery energy support (d).

The maximum required grid energy has fluctuated between 1,866.44 and 2,336.66 MWh, depending on the irradiation values, as shown in Figure 16(a). This demand has decreased to 642.21 MWh and stabilized in July due to the reduced variation in irradiation between minimum and maximum values. The annual dependence on the grid energy has reached up to 18,352.93 MWh in the minimum irradiation scenario. The surplus solar energy sold to the grid has reached 2,375.07 MWh, as indicated in Figure 16(b). However, during the winter months of November and October, no excess solar energy has been available for sale. The PV panels have contributed up to 4,095.24 MWh to the CI operation in the PV/Battery configuration, as shown in June in Figure 16(c). Under minimum irradiation conditions in December, the PV panels have been used exclusively for battery charging during daylight hours. Monthly battery support during the night peaked in December at 182.6 MWh, whereas in May, June, and July, it decreased to 126.72 MWh, as illustrated in Figure 16(d). Figure 17 indicates the annual CO_{2e} of the RE plants, sole grid energy and onboard ship electrification plant utilisation scenarios.

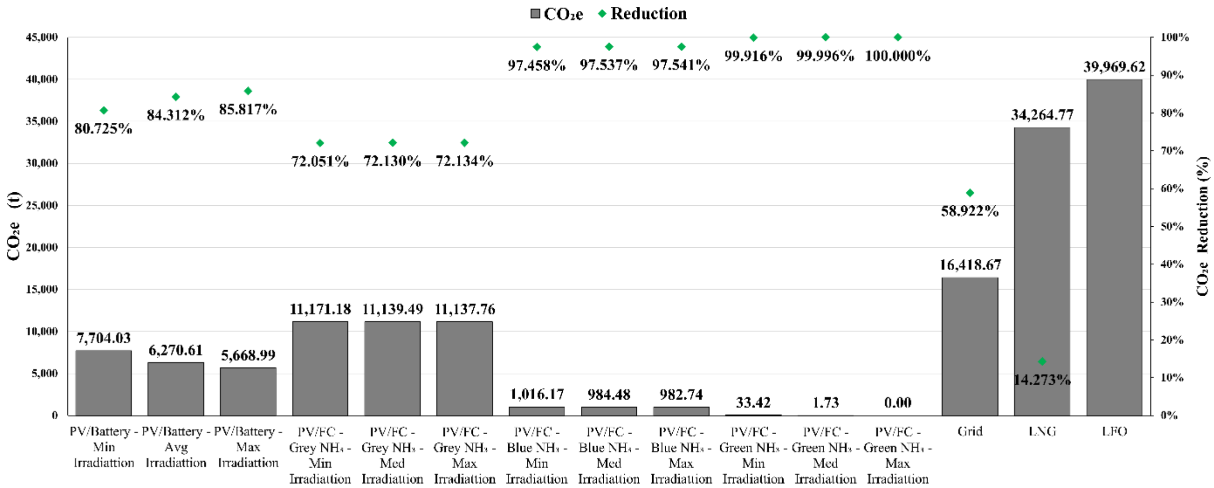

Figure 17. Annual total CO_{2e} and reductions of analysed energy systems.

The LNG utilisation on the ship-side electricity generation for port operations has reduced CO_{2e} by 14.27% which is the lowest among the examined cases. Considering the decarbonisation goals set by IMO, this deduction won't be enough in upcoming years. The retrofitting of AE to DF engines can contribute more in terms of the ship's operational emissions yielding a reduction in CII and EEXI. However, the shore connection usage has provided more environmental advantage in port operations. The sole usage of the national grid for the CI operation has reduced the CO_{2e} by 58.92%. PV/Battery system has provided a reduction between 80.73 and 85.82% depending on the irradiation cases.

The PV/PEMFC plant utilising grey NH_3 has not outperformed the PV/Battery system in terms of CO_{2e} reduction, with rates ranging between 72.05% and 72.134%. However, it has been an improvement over sole LNG usage. The use of blue and green NH_3 as feedstock for H_2 has resulted in a significant reduction in CO_{2e} emissions. Blue NH_3 has eliminated between 97.46% and 97.54% of the annual CO_{2e} emissions from ships during port operations. These reductions have been further amplified by the utilization of green NH_3, which has achieved a decrease ranging from 99.92% to complete elimination (100%) of the annual total CO_{2e} emissions. Table 6 demonstrates the calculated installation, operation, and fuel costs of the configurations.

Table 6. Lifetime $\boldsymbol{C_{plant}}$ and annual $\boldsymbol{C_{O\&M}}$ of the configurations in USD.

Equipment	**PV/PEMFC**		**PV/Battery**		**MDE**		DF	
	C_{plant}	$C_{O\&M}$	C_{plant}	$C_{O\&M}$	C_{plant}	$C_{O\&M}$	C_{plant}	$C_{O\&M}$
PV Panel	1,200,374	12,004	1,200,374	12,004	0	0	0	0
Battery	2,587,423	25,874	51,748,470	517,485	0	0	0	0
PEMFC	25,912,692	388,690	0	0	0	0	0	0
H_2 Storage	9,060,538	90,605	0	0	0	0	0	0
H_2 P&T	16,592,000	663,680	0	0	0	0	0	0
NH_3 P&T and Storage	6,290,472	31,083	0	0	0	0	0	0
Electrolyser	1,280,633	25,613	0	0	0	0	0	0
Balance of System	641,912	12,838	478,202	9,564	0	0	0	0
MPPT	55,517	555	55,517	555	0	0	0	0
HFO Storage	0	0	0	0	598,840	5,988	0	0
LNG Storage	0	0	0	0	0	0	12,920,000	129,200
MDE	0	0	0	0	862,340	12,935	149,710	1,497
DF	0	0	0	0	0	0	1,390,524	20,858
CI Infrastructure	8,875,726	443,786	8,875,726	443,786	0	0	0	0
Total Cost	72,497,287	1,694,729	62,358,288	983,394	1,461,180	18,924	14,460,234	151,555

The operating hours of the PEMFCs have been calculated at 81,833.20 hours. Given the 40,000-hour lifespan of each unit, the PEMFC stacks will require three replacements over the 20-year plant lifetime. As a result, in the PV/PEMFC configuration, they represent the largest cost component (36%), followed by H_2 P&T equipment, and storage (23%), and NH_3 P&T, and tank (12%). In the PV/Battery configuration, the batteries have been actively utilised, necessitating five-lifetime replacements, which has significantly driven up costs. Batteries account for 83% of the installation cost in this configuration. While the conventional MDE system for ships remains the most cost-effective solution in terms of $\boldsymbol{C_{plant}}$, DF engines have also been competitive in terms of pricing. However, the cost of onboard electricity production has increased substantially due to the need for LNG storage and P&T equipment. Involving the operational carbon prices, the annual $\boldsymbol{C_{fuel}}$, annual grid energy expenditures and excess solar energy sold back to the grid have been demonstrated in Table 7.

Table 7. Annual $\boldsymbol{C_{fuel}}$ including carbon price regarding the scenarios in USD.

Annual Fuel Price	**Low**	Medium	High
VLSFO (MDE)	9,185,422	10,308,252	11,279,520
LNG (DF)	7,400,330	8,915,545	10,497,258
Grey NH_3	2,882,715	2,915,473	2,948,231
Blue NH_3	3,695,116	4,189,764	4,690,504
Green NH_3	4,586,137	5,568,881	9,172,274
Surplus Solar Energy Income			
Irradiation Scenarios	Min	Average	Max
PV/ Battery	602,955	1,183,633	1,662,232
PV/PEMFC	2,376,211	3,515,430	4,252,360
Grid Energy Expenditure			
Irradiation Scenarios	Min	Average	Max
PV/ Battery	2,929,834	2,384,706	2,155,912
PV/PEMFC	12,710	659	0

As current carbon pricing has been applied to operational CO_2 emissions, the cost of VLSFO and LNG has been calculated to be higher compared to NH_3 prices. Since NH_3 is widely available for agricultural applications, its price has remained lower than that of marine fuels, particularly when produced via the grey method. The PV/Battery system has generated an average annual income of $1,183,663, with a range between $602,955 and $1,662,232, by selling excess solar energy to the national grid. The PV/PEMFC configuration has earned an average of $3,515,430 annually, with income varying from $2,376,211 to $4,252,360, depending on irradiation levels. The PV/Battery system has required national grid energy purchases ranging between $2,155,912 and $2,929,834, while the PV/PEMFC configuration has needed only $12,710 under the minimum irradiation scenario. Using the energy outcomes and cost calculations, the LCOE for each configuration has been calculated and is presented in Table 8.

Table 8. LCOE of the analysed configurations ($/MWh).

PV/PEMFC Grey NH_3	Irradiation Scenario		
Fuel Scenario	Min	Average	Max
Low	182.33	149.83	129.00
Medium	183.25	150.75	129.93
High	184.18	151.68	130.85
PV/PEMFC Blue NH_3	Irradiation Scenario		
Fuel Scenario	Min	Average	Max
Low	205.26	172.76	151.94
Medium	219.23	186.73	165.90
High	233.36	200.86	180.04
PV/PEMFC Green NH_3	Irradiation Scenario		
Fuel Scenario	Min	Average	Max
Low	230.42	197.92	177.09
Medium	258.16	225.66	204.84
High	359.89	327.39	306.57
	Irradiation Scenario		
	Min	Average	Max
PV/Battery	196.52	181.13	174.67
Grid	186.92		
Fuel Scenario	VLSFO		LNG
Low	262.27		237.10
Medium	293.97		279.88
High	321.39		324.53

The ship electrification unit is more expensive than the CI application, as shown in Table 8. Depending on fuel prices, the LCOE for VLSFO in MDEs has ranged from \$262.27 to \$321.9 per MWh. The use of LNG in DF engines as the primary fuel has demonstrated lower LCOEs than VLSFO in both low and medium-fuel price scenarios, at \$237.10 and \$279.88 per MWh, respectively. However, in the high fuel price case, its LCOE has exceeded that of VLSFO, reaching \$324.53 per MWh.

Overall, the implementation of CI technology has improved the LCOE. The grid-only system has delivered an LCOE of \$186.92 per MWh, which is 36.41% and 33.21% lower than the medium VLSFO and LNG scenarios, respectively. The PV/battery hybrid system has performed comparably to the grid-only system under the average irradiation scenario, with its LCOE found to range between \$174.67 and \$196.52 per MWh, depending on the level of irradiation variation.

The economic performance of the PV/PEMFC scenario has depended on both irradiation and fuel price conditions, resulting in a high degree of variability in LCOE. The Grey NH_3-utilised as the feedstock in the PV/PEMFC system has achieved the lowest LCOE among the analyzed configurations, at \$129 per MWh. However, this value can rise to \$184.18 per MWh under minimum irradiation and maximum fuel price scenarios. The overall LCOE has increased with the use of Blue NH_3, although the PV/PEMFC system utilizing Blue NH_3 as feedstock has exhibited lower LCOE values compared to onboard ship electrification, ranging between \$151.94 and \$233.36 per MWh. Finally, the LCOE of the system using green NH_3 as the H_2 source has ranged from \$177.09 to \$359.89 per MWh. Depending on the future pricing of green NH_3, LCOE values may stabilise toward the lower end of this range. Table 9 presents the simple PBP of the CI configurations, with the tariff set at \$293.97 per MWh, corresponding to the average LCOE of a VLSFO-powered onboard ship electricity generation plant.

Table 9. PBP of the analysed CI configurations in years.

PV/PEMFC Grey NH_3	Irradiation Scenario		
Fuel Scenario	Min	Average	Max
Low	8.84	7.75	7.19
Medium	8.88	7.78	7.21
High	8.91	7.81	7.23
PV/PEMFC Blue NH_3	Irradiation Scenario		
Fuel Scenario	Min	Average	Max
Low	9.81	8.49	7.82
Medium	10.52	9.01	8.26
High	11.34	9.61	8.76
PV/PEMFC Green NH_3	Irradiation Scenario		
Fuel Scenario	Min	Average	Max
Low	11.16	9.48	8.65
Medium	13.15	10.88	9.79
High	37.97	23.69	19.09
	Irradiation Scenario		
	Min	Average	Max
PV/Battery	8.78	7.58	6.98
Grid	2.06		

When national grid electricity has been utilized as the CI source, the PBP has been the shortest, at 2.06 years. The PV/Battery system has demonstrated a PBP ranging from 6.98 to 8.78 years, with an average of 7.58 years, depending on irradiation levels. The PV/PEMFC configuration using Grey NH_3 for H_2 production has exhibited an average PBP of 7.78 years, varying between 7.19 and 8.91 years, depending on fuel prices and irradiation levels. With Blue NH_3 as the feedstock, the mean PBP has increased to 9.01 years, fluctuating between 7.82 and 11.34 years.

In the Green NH_3 scenario, the PBP range has further increased. For low and medium fuel prices, the PBP has been estimated between 8.95 and 13.15 years. However, with high Green NH_3 prices, the selected tariff for the CI application becomes insufficient due to the substantially increased PBPs. The use of Green NH_3 -sourced H_2 in the PV/PEMFC CI application has resulted in an average PBP of 23.69 years, ranging from 19.09 to 37.97 years, depending on irradiation levels.

4. DISCUSSION

The CO_{2e} reduction of the PV/Battery system aligns with similar studies in the literature. This analysis showed a decrease between 80.73% and 85.82%, comparable to findings by Bakar et al. (2022), who reported an 82.51% reduction, and Colarossi and Principi (2023), who calculated a maximum reduction of 87.4%. The proposed PV/PEMFC has not been studied directly however, similar applications validate the outcomes both environmentally and economically. The findings of Coppola and Quaranta (2014) when the economic parameters of the study are updated regarding the 2024 data align with this study's findings. The economic outcomes can be supported by the CI models of Abu Bakar et al. (2024); Colarossi and Principi (2023); Sifakis et al. (2022).

The global implementation of green CI technologies in industrial applications supports the findings of this analysis. For instance, the Port of Los Angeles has successfully integrated green CI applications, leading to a reduction of up to 98% in emissions from berthed ships (Zhang et al., 2024). Similarly, the Port of Hamburg has achieved a 40% reduction in GHG emissions through these measures. The Port of Rotterdam has also adopted renewable energy sources, such as wind power, alongside alternative fuel-powered equipment, further contributing to overall emissions reductions (Kurt, 2023).

Selling excess solar energy back to the grid has significantly improved the economic feasibility of the RE CI systems. Without selling PV electricity to the national grid, the average PBP for the PV/PEMFC system using Grey NH_3 has increased to 12.5 years, representing a 60.59% increment. For Blue NH_3, the PBP has risen to 16.01 years, reflecting a 77.64% increase, and for Green NH_3, the PBP has surged to 23.03 years, marking a 111.65% increment. For the PV/Battery system, the PBP has increased by 16.80%, reaching 8.85 years when excess solar energy is not sold back to the grid. Particularly for the PV/PEMFC system, selling surplus solar energy back to the national grid has substantially enhanced the economic feasibility of the system.

Potential future cost reductions in green and blue NH_3, PEMFC technology, NH_3/H_2 storage and transfer equipment, and electrolysers could further enhance the economic feasibility of the proposed system. Currently, low-carbon H_2 production technologies are still underdeveloped. In the future, it will be crucial to intensify research and development in these technologies, expand production capabilities, and build the necessary infrastructure. These advancements will facilitate the widespread adoption of low-carbon H_2 as a key energy commodity (Capros et al., 2019; Yu et al., 2021). Additionally, Green NH_3 production presents a more environmentally friendly and economically viable alternative to the traditional Haber-Bosch process, particularly when considering improvements in electrolyser energy efficiency, reductions in water electrolyzer costs, and lower LCOE for renewable energy sources (Lee et al., 2022).

Beyond the port investment angle explored in this paper, the system's potential hinges on vessel owners achieving sufficient fuel savings to incentivize the adoption of onboard technology. A key challenge in implementing CI is the considerable investment required from both shipowners and port operators. The substantial costs associated with upgrading port infrastructure and retrofitting vessels represent a major obstacle to the broader adoption of the system (Abu Bakar et al., 2024). The lack of standardisation in the use and safety protocols for H_2 and NH_3 at port facilities has been a significant barrier to the implementation of CI systems (Daniel et al., 2023). While the PV/PEMFC system has reduced reliance on grid energy, the PV/Battery system remains dependent on the national grid, creating an additional challenge in managing interactions during peak load periods. The adoption of an improved power distribution strategy, along with additional investments in national grid stability, would be crucial solutions, though they introduce hidden costs to the CI implementation process (Reusser & Pérez, 2021).

Liquid NH_3, which is H_2-rich and can be stored at ambient temperature and pressure, serves as an excellent medium for H_2 storage.H_2 can be extracted from NH_3 through electrolysis, which theoretically requires less energy compared to water electrolysis. Water electrolysis demands 21 times more energy per gram of H_2 compared to NH_3 electrolysis (Boggs & Botte, 2009). H_2 is expected to eventually replace LNG as a cleaner energy carrier, but transporting pure H_2 remains challenging due to technical limitations. NH_3 offers a practical alternative, with an established distribution network adaptable to new applications. Since NH_3 often serves as an H_2 carrier, it must be converted back to H_2 at the point of use, either at the shore facilities or onboard (Andriani & Bicer, 2023). Solid oxide and proton exchange membrane electrolysers offer potentially higher efficiency for both NH_3 and water electrolysis. However, for large-scale applications, alkaline electrolysers are generally more reliable and better suited (Nami et al., 2024).

5. CONCLUSION

The research paper analysed the two different RE plant designs for the CI application on the reference port facility and compared these designs to onboard electricity generation options and CI using the national grid electricity. The generated energy and H_2 production according to the months were demonstrated. The environmental analysis detected CO_{2e} for each option while LCOE and PBP assessed the economic performance. The main outcomes derived from the study can be listed as follows:

- The use of LNG-DF in the ship's electrification system resulted in a 14.27% reduction in total CO_{2e}, a 90.79% decrease in SO_x emissions, and the complete or near-complete elimination of all other emissions.
- The sole grid energy usage for the CI application led to a reduction in CO_{2e} at 58.92%.
- The PV/PEMFC system, using green NH_3 as the feedstock for H_2, achieved the highest CO_{2e} reduction, ranging from 99.92% to 100.00%, depending on irradiation levels. The PV/PEMFC system with blue NH_3 provided the second-largest CO_{2e} reduction, ensuring a decrease between 97.46% and 97.54%.
- Using grey NH_3 in the PV/PEMFC system led to a CO_{2e} reduction of 72.05% to 72.13%, which falls behind the PV/Battery system, where CO_{2e} reductions ranged from 80.73% to 85.82%.
- National grid energy dependence was 79.58 MWh annually in the minimum irradiation scenario for PV/PEMFC while it was calculated at 18,352.93 MWh under the minimum irradiation for PV/Battery configuration.
- The use of LNG in DF engines showed lower LCOEs than VLSFO in low and medium fuel price scenarios but exceeded VLSFO costs under high fuel prices.
- The implementation of CI technology improved the LCOE, with the grid-only system delivering \$186.92 per MWh, significantly lower than medium VLSFO and LNG scenarios, while the PV/battery hybrid system showed a comparable LCOE ranging from \$174.67 to \$196.52 per MWh depending on irradiation levels.
- The economic performance of the PV/PEMFC system varied significantly based on irradiation and fuel prices, with grey NH_3 achieving the lowest LCOE at \$129 per MWh, rising to \$184.18 under minimum irradation conditions.
- The use of blue NH_3 increased the LCOE to a range of \$151.94 to \$233.36 per MWh, while green NH_3 resulted in the highest LCOE, ranging from \$177.09 to \$359.89 per MWh.
- The shortest PBP of 2.06 years was observed when national grid electricity was used as the CI source.
- The PV/Battery system showed a PBP between 6.98 and 8.78 years, with an average of 7.58 years depending on irradiation levels.
- The PV/PEMFC configuration using grey NH_3 for H_2 production exhibited an average PBP of 7.78 years, varying between 7.19 and 8.91 years, influenced by fuel prices and irradiation.
- With blue NH_3 as the feedstock, the mean PBP increased to 9.01 years, ranging from 7.82 to 11.34 years.
- Green NH_3-sourced H_2 usage in the PV/PEMFC configuration resulted in the longest PBP, averaging 23.69 years and ranging from 19.09 to 37.97 years, depending on irradiation levels.

The limitations of the study can be explained as follows:

- The annual energy demand calculations were based on a consistent monthly energy demand profile, which may not reflect potential seasonal variations.

- It was assumed that the ships' schedules remained unchanged throughout the year, potentially overlooking fluctuations in shipping activity.
- Solar energy computations relied on monthly minimum, average, and maximum irradiation values, as well as average sunrise and sunset times, which may not capture daily variations in solar availability.
- The cost of grid energy and the revenue from selling excess energy back to the grid were assumed to be constant, despite potential market fluctuations.
- H_2 consumption was estimated using PEMFC performance curves, and H_2 production was based on assumptions about the energy needs of electrolysers.
- Operational and upstream coefficients were assumed to remain constant throughout the analysis, not accounting for dynamic changes in operation or supply chain impacts.
- The analysis did not include the scrap value of batteries and PEMFCs, which could affect the overall economic evaluation.

The study's findings offered critical insights for policymakers, port operators, and the shipping industry in advancing global decarbonisation goals. By demonstrating significant CO_{2e} reductions, particularly with green and blue NH_3 in the PV/PEMFC systems, the research highlighted the potential of renewable energy-based CI technologies to dramatically reduce emissions in port facilities. The economic analysis, which revealed competitive LCOEs for grid-only and PV/battery hybrid systems, further supports the adoption of these technologies as cost-effective alternatives to traditional fuel sources, though careful consideration must be given to irradiation and fuel price variability. Policymakers and stakeholders can use these findings to guide investment in RE infrastructure, align with future fuel pricing trends, and prioritise scalable solutions that balance environmental and economic objectives.

Future research could explore the implementation of alternative H_2 production technologies, the evaluation of various FC types, and the integration of additional renewable energy sources such as tidal and wind. It could also focus on optimising equipment sizing by feeding the results of environmental and economic analyses into a metaheuristic algorithm. Additionally, the installation and testing of the proposed system in a pilot project, involving collaboration between industrial and academic partners, would provide valuable practical insights.

ACKNOWLEDGEMENTS
We are grateful to the editor and reviewers for their thorough feedback and insightful comments on an earlier draft of this paper. Their contributions have greatly enhanced the quality of the work.

DISCLAIMER
This paper is the opinion of the authors and does not necessarily represent the belief and policy of their employers.

REFERENCES

Abu Bakar, N. N., Bazmohammadi, N., Vasquez, J. C., & Guerrero, J. M. (2023). Electrification of onshore power systems in maritime transportation towards decarbonization of ports: A review of the cold ironing technology. *Renewable and Sustainable Energy Reviews*, *178*. https://doi.org/10.1016/j.rser.2023.113243

Abu Bakar, N. N., Uyanik, T., Arslanoglu, Y., Vasquez, J. C., & Guerrero, J. M. (2024). Two-stage energy management framework of the cold ironing cooperative with renewable energy for ferry. *Energy Conversion and Management*, *311*. https://doi.org/10.1016/j.enconman.2024.118518

Aijjou, A., Bahatti, L., & Raihani, A. (2019). Influence of Solar Energy on Ship Energy Efficiency: Feeder Container Vessel as Example. *International Journal of Electrical Energy*, *7*(1), 21-25. https://doi.org/10.18178/ijoee.7.1.21-25

Akpinar, E. K. (2006). Mathematical modelling of thin layer drying process under open sun of some aromatic plants. *Journal of Food Engineering*, *77*(4), 864-870. https://doi.org/https://doi.org/10.1016/j.jfoodeng.2005.08.014

Ammar, N. R., & Seddiek, I. S. (2023). Hybrid/dual fuel propulsion systems towards decarbonization: Case study container ship. *Ocean Engineering*, *281*, 114962. https://doi.org/https://doi.org/10.1016/j.oceaneng.2023.114962

Andriani, D., & Bicer, Y. (2023). A Review of Hydrogen Production from Onboard Ammonia Decomposition: Maritime Applications of Concentrated Solar Energy and Boil-Off Gas Recovery. *Fuel*, *352*, 128900-128900. https://doi.org/10.1016/J.FUEL.2023.128900

Atchison, J. (2021). *Producing cheap, clean hydrogen: new updates*. Retrieved 09/07/2024 from https://ammoniaenergy.org/articles/producing-cheap-clean-hydrogen-new-updates/

Babar, P., & Botte, G. G. (2024). Recent Advances in Ammonia Electrolysis for Sustainable Hydrogen Generation. *ACS Sustainable Chemistry & Engineering*, *12*(35), 13030-13047. https://doi.org/10.1021/acssuschemeng.4c02093

Bakar, N. N. A., Guerrero, J. M., C. Vasquez, J., Bazmohammadi, N., Othman, M., Rasmussen, B. D., & Al-Turki, Y. A. (2022). Optimal Configuration and Sizing of Seaport Microgrids including Renewable Energy and Cold Ironing—The Port of Aalborg Case Study. *Energies*, *15*(2). https://doi.org/10.3390/en15020431

Bayraktar, M., Yuksel, O., & Pamik, M. (2023). An evaluation of methanol engine utilization regarding economic and upcoming regulatory requirements for a container ship. *Sustainable Production and Consumption*, *39*, 345-356. https://doi.org/10.1016/j.spc.2023.05.029

Binot, F., Meunier, S., Reinbold, V., Petit, M., Correcher, S., & Mamadou, K. (2024). Optimization of the design of photovoltaic-based seaport microgrids considering techno-economic and environmental criteria. *Energy Reports*, *11*, 5819-5830. https://doi.org/https://doi.org/10.1016/j.egyr.2024.05.053

Boggs, B. K., & Botte, G. G. (2009). On-board hydrogen storage and production: An application of ammonia electrolysis. *Journal of Power Sources*, *192*(2), 573-581. https://doi.org/10.1016/J.JPOWSOUR.2009.03.018

Burges, J. (2024). *Blue, green ammonia prices diverge as electrolysis power prices rise, natural gas falls*. Retrieved 09/07/2024 from https://www.spglobal.com/commodityinsights/en/market-insights/latest-news/energy-transition/031924-blue-green-ammonia-prices-diverge-as-electrolysis-power-prices-rise-natural-gas-falls

Canepa, M., Ballini, F., Dalaklis, D., Frugone, G., & Sciutto, D. (2023). Cold Ironing: Socio-Economic Analysis in the Port of Genoa. *Logistics*, *7*(2). https://doi.org/10.3390/logistics7020028

Caprara, G., Armas, V., Sousa, D. d. M., Kermani, M., & Martirano, L. (2021, 7-10 Sept. 2021). An Energy Storage System to support Cruise Ships Cold Ironing in the Port of Civitavecchia. 2021 IEEE International Conference on Environment and Electrical Engineering and 2021 IEEE Industrial and Commercial Power Systems Europe (EEEIC / I&CPS Europe),

Caprara, G., Martirano, L., Kermani, M., Sousa, D. d. M. e., Barilli, R., & Armas, V. (2022, 28 June-1 July 2022). Cold Ironing and Battery Energy Storage System in the Port of Civitavecchia. 2022 IEEE International Conference on Environment and Electrical Engineering and 2022 IEEE Industrial and Commercial Power Systems Europe (EEEIC / I&CPS Europe),

Capros, P., Zazias, G., Evangelopoulou, S., Kannavou, M., Fotiou, T., Siskos, P., De Vita, A., & Sakellaris, K. (2019). Energy-system modelling of the EU strategy towards climate-neutrality. *Energy Policy*, *134*, 110960. https://doi.org/https://doi.org/10.1016/j.enpol.2019.110960

CarbonFootPrint. (2023). *COUNTRY SPECIFIC ELECTRICITY GRID GREENHOUSE GAS EMISSION FACTORS*. Retrieved 21/06/2024 from https://www.carbonfootprint.com/docs/2023_02_emissions_factors_sources_for_2022_electricity_v10.pdf

Colak, E., Aksoy, H., & Sanli, B. (2021). *Techno-economic study of Turkey's production and export potential for green hydrogen* (978-625-7329-56-9). S. University.

Colarossi, D., & Principi, P. (2023). Optimal sizing of a photovoltaic/energy storage/cold ironing system: Life Cycle cost approach and environmental analysis. *Energy Conversion and Management*, *291*. https://doi.org/10.1016/j.enconman.2023.117255

Coppola, T., & Quaranta, F. (2014). *Fuel saving and reduction of emissions in ports with cold ironing applications* Proceedings of the high speed marine vehicle conference, Naples, Italy.

CORDIS. (2019). *Final Report Summary - STAYERS (STAYERSStationary PEM fuel cells with lifetimes beyond five years)*. https://cordis.europa.eu/project/id/256721/reporting

Daniel, H., Antunes, C. H., Trovão, J. P. F., & Williams, D. (2023). Shore operations enhancement of bulk carriers based on a multi-objective sizing approach. *Energy Conversion and Management*, *276*, 116497. https://doi.org/https://doi.org/10.1016/j.enconman.2022.116497

DNV. (2024). *IMO GHG strategy*. Retrieved 14/07/2024 from https://www.dnv.com/maritime/hub/decarbonize-shipping/key-drivers/regulations/imo-regulations/ghg-vision/

Edwardes-Evans, H., Perez, M., & Burges, J. (2024). *Interactive: Platts Ammonia price chart*. Retrieved 24/09/2024 from https://www.spglobal.com/commodityinsights/en/market-insights/latest-news/energy-transition/051023-interactive-ammonia-price-chart-natural-gas-feedstock-europe-usgc-black-sea

El-Khozondar, H. J., El-Batta, F., El-Khozondar, R. J., Nassar, Y., Alramlawi, M., & Alsadi, S. (2022). Standalone hybrid PV/wind/diesel-electric generator system for a COVID-19 quarantine center. *Environ Prog Sustain Energy*, e14049. https://doi.org/10.1002/ep.14049

Enea, D., & Mastrilli, A. (2024). Sustainable planning: the case study of the Strait of Messina ports. *Environmental Science and Pollution Research*, *31*(10), 15348-15363. https://doi.org/10.1007/s11356-023-31764-2

Esen, H., Inalli, M., Esen, M., & Pihtili, K. (2007). Energy and exergy analysis of a ground-coupled heat pump system with two horizontal ground heat exchangers. *Building and Environment*, *42*(10), 3606-3615. https://doi.org/https://doi.org/10.1016/j.buildenv.2006.10.014

Esen, M., & Yuksel, T. (2013). Experimental evaluation of using various renewable energy sources for heating a greenhouse. *Energy and Buildings*, *65*, 340-351. https://doi.org/https://doi.org/10.1016/j.enbuild.2013.06.018

EuropeanCommission. (2024). *Reducing emissions from the shipping sector.* . Retrieved 14/07/2024 from https://climate.ec.europa.eu/eu-action/transport/reducing-emissions-shipping-sector_en

Fang, Q., Blum, L., & Stolten, D. (2019). Electrochemical Performance and Degradation Analysis of an SOFC Short Stack Following Operation of More than 100,000 Hours. *Journal of The Electrochemical Society*, *166*(16), F1320-F1325. https://doi.org/10.1149/2.0751916jes

Frković, L., Ćosić, B., Falkoni, A., Pukšec, T., & Vladimir, N. (2024). Shore-to-ship: Enabling the electrification sustainability of maritime transport with the nexus between berthed cruise ships and renewables in the isolated energy systems. *Ocean Engineering*, *302*, 117537. https://doi.org/https://doi.org/10.1016/j.oceaneng.2024.117537

Gilbert, P., Walsh, C., Traut, M., Kesieme, U., Pazouki, K., & Murphy, A. (2018). Assessment of full life-cycle air emissions of alternative shipping fuels. *Journal of Cleaner Production*, *172*, 855-866. https://doi.org/https://doi.org/10.1016/j.jclepro.2017.10.165

Glavinović, R., Krčum, M., Vukić, L., & Karin, I. (2023). Cold Ironing Implementation Overview in European Ports—Case Study—Croatian Ports. *Sustainability*, *15*(11). https://doi.org/10.3390/su15118472

GovUK. (2022). *Category A project supported: Gemlik Gübre Sanayii A.Ş., Urea production plant project, Turkey*. Retrieved 23/09/2024 from https://www.gov.uk/government/publications/category-a-project-supported-gemlik-gubre-sanayii-as-urea-production-plant-project-turkey/category-a-project-supported-gemlik-gubre-sanayii-as-urea-production-plant-project-turkey

Gülmez, Y., Konur, O., Yüksel, O., & Korkmaz, S. A. (2024). Comparative Economic Assessment of On-Grid Solar Power System Applications Having Limited Areas: A Case Study on a Shore Facility. *Environmental Modeling & Assessment*, *29*(4), 667-681. https://doi.org/10.1007/s10666-023-09949-3

Hanada, N., Hino, S., Ichikawa, T., Suzuki, H., Takai, K., & Kojima, Y. (2010). Hydrogen generation by electrolysis of liquid ammonia. *Chem Commun (Camb)*, *46*(41), 7775-7777. https://doi.org/10.1039/c0cc01982h

Hansen, K. (2019). Decision-making based on energy costs: Comparing levelized cost of energy and energy system costs. *Energy Strategy Reviews*, *24*, 68-82. https://doi.org/https://doi.org/10.1016/j.esr.2019.02.003

Hatzell, M. C. (2024). The Colors of Ammonia. *ACS Energy Letters*, *9*(6), 2920-2921. https://doi.org/10.1021/acsenergylett.4c01391

Hazar, C., Yuksel, O., & Bayraktar, M. (2023, 14/15 December 2023). *THE COST ANALYSIS AND EVALUATION OF SCRUBBER INVESTMENTS FOR SHIP INSTALLATION* DEU INTERNATIONAL SYMPOSIUM SERIES ONGRADUATE RESEARCHES-2023 Maritime Science & Technology, Izmir.

IEA. (2020). *Projected Costs of Generating Electricity*. Retrieved 27/06/2024 from https://www.oecd-nea.org/upload/docs/application/pdf/2020-12/egc-2020_2020-12-09_18-26-46_781.pdf

IGSAS. (2022). *IGSAS Kocaeli Plant*. Retrieved 25/09/2024 from https://www.yildiz.com/en/our-activity-areas/fertilizer-industry/igsas-kocaeli-plant#:~:text=Producing%20ammoniac%20and%20composite%20fertilizer,fertilizer%20needs%20of%20Turkish%20growers.

IMO. (2023). *GUIDELINES ON LIFE CYCLE GHG INTENSITY OF MARINE FUELS TY OF MARINE FUELS (LCA GUIDELINES)*. Retrieved 23/05/2024 from https://wwwcdn.imo.org/localresources/en/OurWork/Environment/Documents/annex/MEPC%2080/Annex%2014.pdf

Inal, E., & Down, C. (2020). *Turkey take the winding road to solar success*. Retrieved 25/06/2024 from https://www.nortonrosefulbright.com/en-lu/knowledge/publications/4e5c0606/turkey-take-the-winding-road-to-solar-success

Inanc, S. (2024). *En Güncel Elektrik Birim Fiyatları (Temmuz-2024)*. Retrieved 10/07/2024 from https://enerjiajansi.com.tr/elektrik-birim-fiyatlari/

Innes, A., & Monios, J. (2018). Identifying the unique challenges of installing cold ironing at small and medium ports – The case of aberdeen. *Transportation Research Part D: Transport and Environment*, *62*, 298-313. https://doi.org/10.1016/j.trd.2018.02.004

JNGE. (2022). *MPPT solar charge controller.* Retrieved 09/07/2024 from https://www.hfjnge.com/24v-48v-96v-120v-192v-216v-240v-360v-384v-480v-584vhigh-voltage-mppt-solar-charge-controller_p107.html

Kelmalis, A., Dimou, A., Lekkas, D. F., & Vakalis, S. (2024). Cold Ironing and the Study of RES Utilization for Maritime Electrification on Lesvos Island Port. *Environments*, *11*(4). https://doi.org/10.3390/environments11040084

Kılıç, A., Yolcu, M., Kılıç, F., & Bilgili, L. (2020). Assessment of ship emissions through cold ironing method for Iskenderun Port of Turkey. *Environmental Research and Technology*, *3*(4), 193-201. https://doi.org/10.35208/ert.794595

Kim, J., Huh, C., & Seo, Y. (2022). End-to-end value chain analysis of isolated renewable energy using hydrogen and ammonia energy carrier. *Energy Conversion and Management*, *254*, 115247. https://doi.org/https://doi.org/10.1016/j.enconman.2022.115247

Konur, O., Yuksel, O., Korkmaz, S. A., Colpan, C. O., Saatcioglu, O. Y., & Muslu, I. (2022). Thermal design and analysis of an organic rankine cycle system utilizing the main engine and cargo oil pump turbine based waste heats in a large tanker ship. *Journal of Cleaner Production*, *368*. https://doi.org/10.1016/j.jclepro.2022.133230

Korkmaz, S. A., Erginer, K. E., Yuksel, O., Konur, O., & Colpan, C. O. (2023). Environmental and economic analyses of fuel cell and battery-based hybrid systems utilized as auxiliary power units on a chemical tanker vessel. *International Journal of Hydrogen Energy*, *48*(60), 23279-23295. https://doi.org/10.1016/j.ijhydene.2023.01.320

Kuittinen, N., Heikkilä, M., & Lehtoranta, K. (2023). *REVIEW OF METHANE SLIP FROM LNG ENGINES* (GREEN RAY, Issue. https://greenray-project.eu/wp-content/uploads/2023/04/D1.1_Review_of_methane_slip_from_LNG_engines.pdf

Kurt, İ. (2023). Evaluation of the Green Port Concept for Decarbonized Maritime Industry. In B. Zincir, P. C. Shukla, & A. K. Agarwal (Eds.), *Decarbonization of Maritime Transport* (pp. 157-176). Springer Nature Singapore. https://doi.org/10.1007/978-981-99-1677-1_9

Kuzu, S. L., Bilgili, L., & Kiliç, A. (2021). Estimation and dispersion analysis of shipping emissions in Bandirma Port, Turkey. *Environment, Development and Sustainability*, *23*(7), 10288-10308. https://doi.org/10.1007/s10668-020-01057-6

Lan, H., Wang, X., Hao, W., Hao, D., He, Y., & Xu, N. (2022). Research on the hydrogen consumption of fuel cell electric vehicles based on the flowmeter and short-cut method. *Energy Reports*, *8*, 40-50. https://doi.org/https://doi.org/10.1016/j.egyr.2022.09.091

Lee, B., Winter, L. R., Lee, H., Lim, D., Lim, H., & Elimelech, M. (2022). Pathways to a Green Ammonia Future. *ACS Energy Letters*, *7*(9), 3032-3038. https://doi.org/10.1021/acsenergylett.2c01615

Little, D. J., Smith, I. I. I. M. R., & Hamann, T. W. (2015). Electrolysis of liquid ammonia for hydrogen generation. *Energy & Environmental Science*, *8*(9), 2775-2781. https://doi.org/10.1039/c5ee01840d

Maxwell, C. (2024). *Cost Indices*. Retrieved 25/06/2024 from https://toweringskills.com/financial-analysis/cost-indices/

Nami, H., Hendriksen, P. V., & Frandsen, H. L. (2024). Green ammonia production using current and emerging electrolysis technologies. *Renewable and Sustainable Energy Reviews*, *199*, 114517. https://doi.org/https://doi.org/10.1016/j.rser.2024.114517

Panasonic. (2022). *Specifications for NCR18650GA*. Retrieved 01/05/2024 from https://www.orbtronic.com/content/Datasheet-specs-Sanyo-Panasonic-NCR18650GA-3500mah.pdf

Piccoli, T., Fermeglia, M., Bosich, D., Bevilacqua, P., & Sulligoi, G. (2021). Environmental Assessment and Regulatory Aspects of Cold Ironing Planning for a Maritime Route in the Adriatic Sea. *Energies*, *14*(18). https://doi.org/10.3390/en14185836

PowerCellGroup. (2024). *Marine System 200*. Retrieved 01/05/2024 from https://powercellgroup.com/product/marine-system-200/

Prousalidis, J., Antonopoulos, G., Patsios, C., Greig, A., & Bucknall, R. (2014, 2-5 Sept. 2014). Green shipping in emission controlled areas: Combining smart grids and cold ironing. 2014 International Conference on Electrical Machines (ICEM),

Qiu, J., Tao, Y., Lai, S., & Zhao, J. (2022). Pricing Strategy of Cold Ironing Services for All-Electric Ships Based on Carbon Integrated Electricity Price. *IEEE Transactions on Sustainable Energy*, *13*(3), 1553-1565. https://doi.org/10.1109/TSTE.2022.3157645

Reusser, C. A., & Pérez, J. R. (2021). Evaluation of the Emission Impact of Cold-Ironing Power Systems, Using a Bi-Directional Power Flow Control Strategy. *Sustainability*, *13*(1).

Rivarolo, M., Riveros-Godoy, G., Magistri, L., & Massardo, A. F. (2019). Clean Hydrogen and Ammonia Synthesis in Paraguay from the Itaipu 14 GW Hydroelectric Plant. *ChemEngineering*, *3*(4). https://doi.org/10.3390/chemengineering3040087

Rouwenhorst, K. (2023). *Technology status: alkaline electrolysis for renewable ammonia production*. Retrieved 25/09/2024 from https://ammoniaenergy.org/articles/technology-status-alkaline-electrolysis-for-renewable-ammonia-production/

Saxena, S., Hendricks, C., & Pecht, M. (2016). Cycle life testing and modeling of graphite/LiCoO2 cells under different state of charge ranges. *Journal of Power Sources*, *327*, 394-400. https://doi.org/https://doi.org/10.1016/j.jpowsour.2016.07.057

Şenol, Y. E., & Seyhan, A. (2024). Renewable energy-based electrical microgrid of cold ironing energy supply for berthed ships [Gemiler için sahil elektriği tedarikinde yenilenebilir enerji tabanlı mikro şebeke uygulaması]. *Turkish Journal of Maritime and Marine Sciences*, *10*(1), 14-26. https://doi.org/10.52998/trjmms.1372732

Seo, Y., & Han, S. J. (2021). Economic Evaluation of an Ammonia-Fueled Ammonia Carrier Depending on Methods of Ammonia Fuel Storage. *Energies*, *14*(24), Article 8326. https://doi.org/10.3390/en14248326

Seyhan, A., Ay, C., & Deniz, C. (2023). Evaluating the emission reduction efficiency of automatic mooring system and cold ironing: the case of a port in Izmit Bay. *Australian Journal of Maritime & Ocean Affairs*, *15*(2), 227-245. https://doi.org/10.1080/18366503.2022.2038465

ShipandBunker. (2024a). *EU-ETS Understanding the EU's Emissions Trading System for Shipping*. Retrieved 25/06/2024 from https://shipandbunker.com/eu-ets

ShipandBunker. (2024b). *World Bunker Prices*. Retrieved 25/06/2024 from https://shipandbunker.com/prices

Shu, G., Liu, P., Tian, H., Wang, X., & Jing, D. (2017). Operational profile based thermal-economic analysis on an Organic Rankine cycle using for harvesting marine engine's exhaust waste heat. *Energy Conversion and Management*, *146*, 107-123. https://doi.org/https://doi.org/10.1016/j.enconman.2017.04.099

Sifakis, N., Vichos, E., Smaragdakis, A., Zoulias, E., & Tsoutsos, T. (2022). Introducing the cold-ironing technique and a hydrogen-based hybrid renewable energy system into ports. *International Journal of Energy Research*, *46*(14), 20303-20323. https://doi.org/10.1002/er.8059

SMA. (2021). *SUNNY CENTRAL STORAGE*. Retrieved 23/05/2024 from https://files.sma.de/assets/275864.pdf

Taner, T. (2015). Optimisation processes of energy efficiency for a drying plant: A case of study for Turkey. *Applied Thermal Engineering*, *80*, 247-260. https://doi.org/10.1016/j.applthermaleng.2015.01.076

Taner, T., & Sivrioglu, M. (2015). Energy–exergy analysis and optimisation of a model sugar factory in Turkey. *Energy*, *93*, 641-654. https://doi.org/https://doi.org/10.1016/j.energy.2015.09.007

Taner, T., & Sivrioglu, M. (2017). A techno-economic & cost analysis of a turbine power plant: A case study for sugar plant. *Renewable and Sustainable Energy Reviews*, *78*, 722-730. https://doi.org/https://doi.org/10.1016/j.rser.2017.04.104

Tang, R., Wu, Z., & Li, X. (2018). Optimal operation of photovoltaic/battery/diesel/cold-ironing hybrid energy system for maritime application. *Energy*, *162*, 697-714. https://doi.org/10.1016/j.energy.2018.08.048

Terlouw, T., Bauer, C., McKenna, R., & Mazzotti, M. (2022). Large-scale hydrogen production via water electrolysis: a techno-economic and environmental assessment. *Energy & Environmental Science*, *15*(9), 3583-3602. https://doi.org/10.1039/d2ee01023b

Tian, Z., Zeng, W., Gu, B., Zhang, Y., & Yuan, X. (2021). Energy, exergy, and economic (3E) analysis of an organic Rankine cycle using zeotropic mixtures based on marine engine waste heat and LNG cold energy. *Energy Conversion and Management*, *228*, 113657. https://doi.org/https://doi.org/10.1016/j.enconman.2020.113657

TommaTech. (2023). *Tommatech TOPCON MonoCrystalline 120TN10*. Retrieved 09/07/2024 from https://cw-enerji.com/en/product/tommatech-460wp-120tn-m10-topcon-solar-panel-1305.html

UNCTAD. (2023). *Review of Maritime Transport 2023. Towards a green and just transition*. Retrieved 03/05/2024 from https://unctad.org/publication/review-maritime-transport-2023

Urrejola, E., Antonanzas, J., Ayala, P., Salgado, M., Ramírez-Sagner, G., Cortés, C., Pino, A., & Escobar, R. (2016). Effect of soiling and sunlight exposure on the performance ratio of photovoltaic technologies in Santiago, Chile. *Energy Conversion and Management*, *114*, 338-347. https://doi.org/https://doi.org/10.1016/j.enconman.2016.02.016

Vahabzad, N., Mohammadi-Ivatloo, B., & Anvari-Moghaddam, A. (2021). Optimal energy scheduling of a solar-based hybrid ship considering cold-ironing facilities. *IET Renewable Power Generation*, *15*(3), 532-547. https://doi.org/https://doi.org/10.1049/rpg2.12015

Vakili, S., & Ölçer, A. I. (2023). Techno-economic-environmental feasibility of photovoltaic, wind and hybrid electrification systems for stand-alone and grid-connected port electrification in the Philippines. *Sustainable Cities and Society*, *96*, 104618. https://doi.org/https://doi.org/10.1016/j.scs.2023.104618

Vitse, F., Cooper, M., & Botte, G. G. (2005). On the use of ammonia electrolysis for hydrogen production. *Journal of Power Sources*, *142*(1), 18-26. https://doi.org/https://doi.org/10.1016/j.jpowsour.2004.09.043

Wang, Y., Pang, Y., Xu, H., Martinez, A., & Chen, K. S. (2022). PEM Fuel cell and electrolysis cell technologies and hydrogen infrastructure development – a review. *Energy & Environmental Science*, *15*(6), 2288-2328. https://doi.org/10.1039/d2ee00790h

Wartsila. (2024). *Cold Ironing*. Retrieved 14/07/2024 from https://www.wartsila.com/encyclopedia/term/cold-ironing

Wärtsilä. (2024). *Online engine configurator - Find the right ship engine for you*. Retrieved 29/04/2024 from https://www.wartsila.com/marine/engine-configurator

WeatherSpark. (2024). *Climate and Average Weather Year Round in İzmit*. Retrieved 21/06/2024 from https://weatherspark.com/y/96028/Average-Weather-in-%C4%B0zmit-Turkey-Year-Round

Yfantis, E., Paradeisiotis, A., Ioannou, C., Mallouppas, G., Ktoris, A., & Damianou, S. (2023, 5-8 June 2023). Integrated Ship Energy Flowchart: Auxiliary Energy Demand and Shore-Side Electricity. OCEANS 2023 - Limerick, Yu, M., Wang, K., & Vredenburg, H. (2021). Insights into low-carbon hydrogen production methods: Green, blue and aqua hydrogen. *International Journal of Hydrogen Energy*, *46*(41), 21261-21273. https://doi.org/https://doi.org/10.1016/j.ijhydene.2021.04.016

Yuksel, O. (2023). A comprehensive feasibility analysis of dual-fuel engines and solid oxide fuel cells on a tanker ship considering environmental, economic, and regulation aspects. *Sustainable Production and Consumption*, *42*, 106-124. https://doi.org/10.1016/j.spc.2023.09.012

Yüksel, O., Göksu, B., & Bayraktar, M. (2024). Propulsion and photovoltaic charging system parameter computation for an all-electric boat. *Ships and Offshore Structures*, *19*(5), 580-593. https://doi.org/10.1080/17445302.2023.2195239

Yuksel, O., Konur, O., Pamik, M., & Bayraktar, M. (2024). The economic and environmental assessment of alternative marine fuels and nuclear energy utilization on a floating power plant. *Environ Sci Pollut Res Int*. https://doi.org/10.1007/s11356-024-34532-y

Yuksel, O., & Koseoglu, B. (2023). Numerical simulation of the hybrid ship power distribution system and an analysis of its emission reduction potential. *Ships and Offshore Structures*, *18*(1), 78-94. https://doi.org/10.1080/17445302.2022.2028435

Yüksel, O., & Köseoğlu, B. (2022). Regression Modelling Estimation of Marine Diesel Generator Fuel Consumption and Emissions. *Transactions on Maritime Science*, *11*(1), 79-94. https://doi.org/10.7225/toms.v11.n01.w08

Zarabi Golkhatmi, S., Asghar, M. I., & Lund, P. D. (2022). A review on solid oxide fuel cell durability: Latest progress, mechanisms, and study tools. *Renewable and Sustainable Energy Reviews*, *161*, 112339. https://doi.org/https://doi.org/10.1016/j.rser.2022.112339

Zhang, L., Zeng, Q., & Wang, L. (2024). How to Achieve Comprehensive Carbon Emission Reduction in Ports? A Systematic Review. *Journal of Marine Science and Engineering*, *12*(5).